Geological Society of America
Special Paper 419
2007

Geochronologic constraints across the Main Central Thrust shear zone, Bhagirathi River (NW India): Implications for Himalayan tectonics

Elizabeth J. Catlos
School of Geology, Oklahoma State University, Stillwater, Oklahoma 74078, USA

Chandra Shekhar Dubey
Department of Geology, University of Delhi, Delhi, 110007, India

Richard A. Marston
Department of Geography, Kansas State University, Manhattan, Kansas 66506-2904, USA

T. Mark Harrison
Department of Earth and Space Sciences, University of California, Los Angeles, California, 90095-1567, USA

ABSTRACT

The Main Central Thrust shear zone is the dominant crustal thickening feature in the Himalayas, largely responsible for the extreme relief and mass wasting of the range. Along the Bhagirathi River in NW India, the Main Central Thrust is several kilometers thick and separates high-grade gneisses of the Greater Himalayan Crystallines from Lesser Himalayan metasedimentary rocks. Th-Pb ion microprobe ages of monazite dated in rock thin section from the Greater Himalayan Crystallines are Eocene (38.0 ± 0.8 Ma) to Miocene (19.5 ± 0.3 Ma), consistent with the burial of the unit during imbrication of the northern Indian margin and subsequent exhumation due to Main Central Thrust activity, respectively. However, two samples directly beneath the Main Central Thrust yield 4.5 ± 1.1 Ma (T = 540 ± 25 °C and P = 700 ± 180 MPa from coexisting assemblage) and 4.3 ± 0.1 Ma (five grains) matrix monazite ages, suggesting Pliocene reactivation of the structure. Hydrothermal monazites at the base of the Main Central Thrust shear zone record Th-Pb ages of 1.0 ± 0.5 Ma and 0.8 ± 0.2 Ma, the youngest ever reported for the Himalayas. These ages postdate or overlap activity along structures closer to the Indian foreland and show that the zone of Indo-Asia plate convergence did not shift systematically southwestward from the Main Central Thrust toward the foreland during the mountain-building process. Instead, age data support out-of-sequence thrusting and reactivation consistent with critical-taper wedge models of the Himalayas.

Keywords: Himalayas, monazite, geochronology, Main Central Thrust, metamorphism.

Catlos, E.J., Dubey, C.S., Marston, R.A., and Harrison, T.M., 2007, Geochronologic constraints across the Main Central Thrust shear zone, Bhagirathi River (NW India): Implications for Himalayan tectonics, *in* Cloos, M., Carlson, W.D., Gilbert, M.C., Liou, J.G., and Sorensen, S.S., eds., Convergent Margin Terranes and Associated Regions: A Tribute to W.G. Ernst: Geological Society of America Special Paper 419, p. 135–151, doi: 10.1130/2006.2419(07).

INTRODUCTION AND GEOLOGIC BACKGROUND

The Himalayan mountain range was created by the collision of India and Asia, which began during the Late Cretaceous (Figs. 1 and 2) (e.g., Yin and Harrison, 2000). The range is characterized by the presence of five laterally continuous large-scale structures that separate similar lithologies along its entire ~2400 km length (e.g., Le Fort, 1996; Harrison et al., 1999; Upreti, 1999; Hodges, 2000). In the north, the Indus-Tsangpo suture zone separates Asian metasedimentary and igneous rocks from Indian shelf sediments (Tethys Formation) (e.g., Beck et al., 1996; Yin et al., 1999). The South Tibetan Detachment System separates the Tethys Formation from a unit of kyanite- to sillimanite-grade gneisses termed the Greater Himalayan Crystallines (e.g., Burg et al., 1984; Burchfiel et al., 1992). The Main Central Thrust separates the Greater Himalayan Crystallines from Middle Proterozoic phyllites, metaquartzites, and mylonitic augen gneisses of the Lesser Himalayan Formations (e.g., Arita, 1983; Pêcher, 1989; Catlos et al., 2001; Martin et al., 2005). At most locations, rocks within the footwall of the Main Central Thrust show "inverted metamorphism," an increase in metamorphic grade toward structurally shallower levels (e.g., Arita, 1983; Pêcher, 1989; Catlos et al., 2001).

Farther south, the Main Boundary Thrust juxtaposes Lesser Himalayan metasediments from a Neogene molasse termed the Siwalik Formation (e.g., Seeber et al., 1981; Valdiya, 1992; Meigs et al., 1995). South of the Main Boundary Thrust, the Main Frontal Thrust is the boundary between the Siwalik and northern Indo-Gangetic Plains (e.g., Lavé and Avouac, 2000). The Main Frontal Thrust cuts Siwalik strata in places but is also manifested as anticline growth (e.g., Yeats et al., 1992; Powers et al., 1998). These large-scale Himalayan structures sole at depth into a presently active décollement termed the Main Himalayan Thrust (Fig. 2) (e.g., Nelson et al., 1996; Berger et al., 2004).

In addition to these structural elements, the range is characterized by roughly parallel chains of igneous intrusions termed the North Himalayan granites and High Himalayan leucogranites (Figs. 1 and 2) (e.g., Le Fort, 1986; Harris et al., 1993; Harrison et al., 1997). The North Himalayan granites are typically found as plutons within the Tethys Formation, whereas the High Himalayan leucogranites form a large-scale injection complex throughout the structurally higher levels of the Greater Himalayan Crystallines, coalescing as sheet-like plutons near the South Tibetan Detachment System.

Numerous models for the evolution of the Himalayas assume that convergence between the Indian and Asian plates

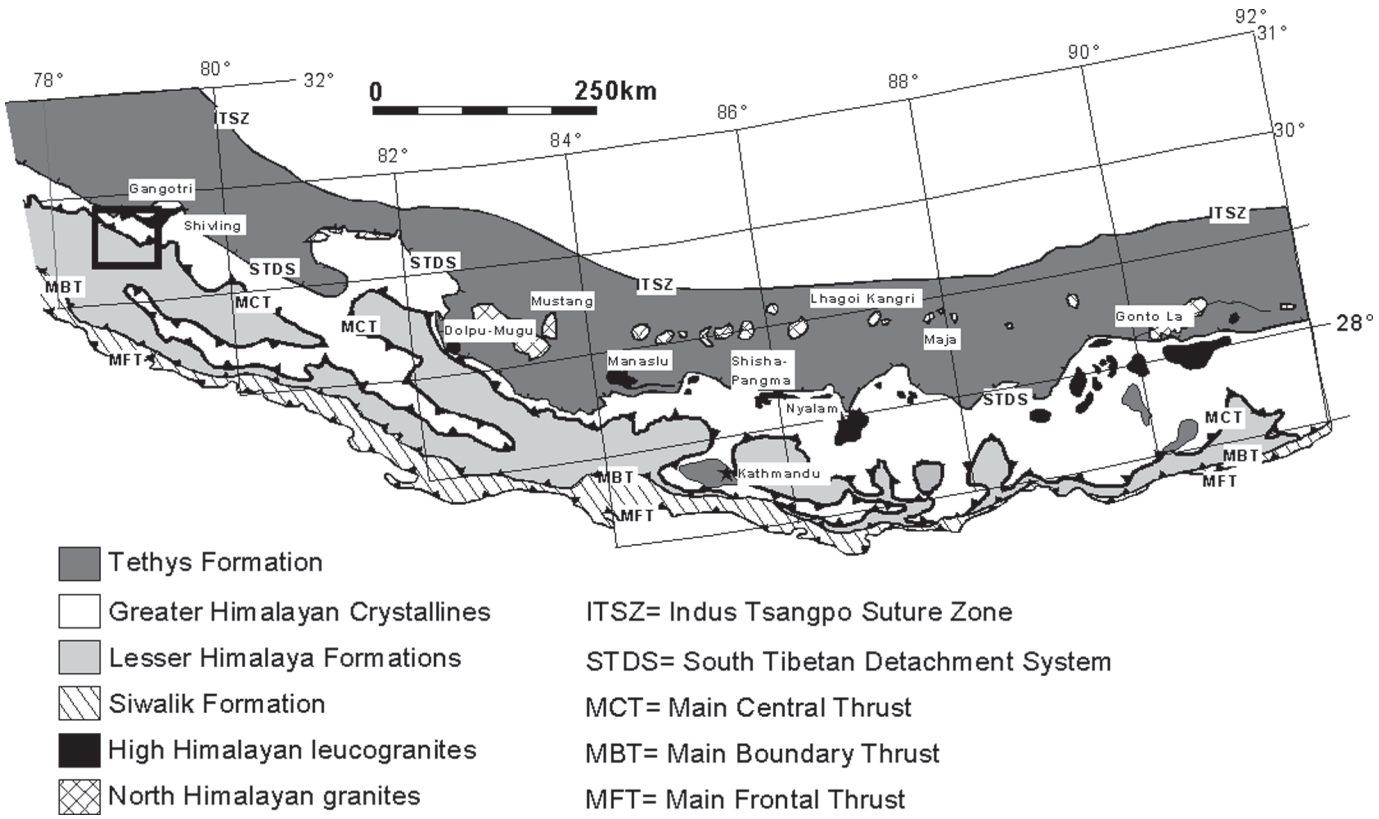

Figure 1. Generalized geological map of the Himalayas after Le Fort (1996). The box outlines the boundary of the study area in NW India. Names of some of the High Himalayan and North Himalayan granites are included for reference.

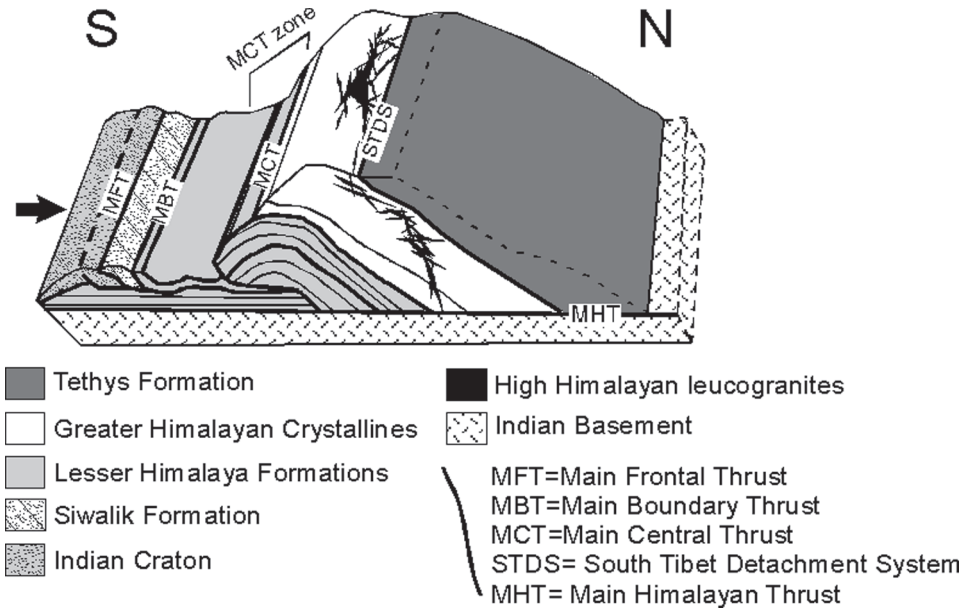

Figure 2. Three-dimensional schematic cartoon of the Himalayas based on the cross section of Schelling and Arita (1991).

was accommodated in a progressive way by large-scale thrusts operating at independent times during the mountain-building process. According to such models, subsequent to activity along the Indus-Tsangpo suture zone during the Late Cretaceous, the intracontinental Main Central Thrust initiated during the early Miocene (e.g., Schelling and Arita, 1991; Vannay and Steck, 1995; Hodges et al., 1996; Stephenson et al., 2001). Zircon and monazite grains within the High Himalayan leucogranites yield early Miocene ages (e.g., Noble and Searle, 1995; Harrison et al., 1997; Searle et al., 1997); thus many models link their origin to decompression melting of the kyanite-grade formations of the Greater Himalayan Crystallines due to slip along the South Tibetan Detachment System (e.g., Harris et al., 1993, 2004; Harris and Massey, 1994). After accommodating ~140–210 km of Indo-Asia convergence (e.g., Schelling and Arita, 1991; Srivastava and Mitra, 1994), the Main Central Thrust ceases activity and the Main Boundary Thrust becomes active during the late Miocene to Pliocene (e.g., Meigs et al., 1995; Brozovic and Burbank, 2000; DeCelles et al., 2001). During the Pliocene to present times, the Main Frontal Thrust is active (e.g., Yeats et al., 1992; Lavé and Avouac, 2000; Jouanne et al., 2004). In this scenario of Himalayan construction, the Main Himalayan Thrust (Fig. 2) and the entire range was created by the successive emplacement of nappes.

Although this "in-sequence" model (Seeber and Gornitz, 1983) has been the foundation upon which many ideas of Himalayan orogenesis and broader continental collision processes have developed (e.g., Le Fort, 1975; Searle and Rex, 1989; England et al., 1992; England and Molnar, 1993; Royden, 1993; Hubbard, 1996), the idea of an inactive Main Central Thrust since the early Miocene has led to several questions, including its persistence as a prominent topographic break between the sea-level Indian craton and the ~5 km high Tibetan Plateau (Fielding, 1996) and the origin of the apparent inverted metamorphic gradient found in its footwall.

An alternative to the "in-sequence" model was developed by exploring the analog of ocean-continent collision, in which a topographic wedge develops between a subducting oceanic slab and overriding continental plate. During ocean-continent collision, the accretionary wedge experiences synchronous thrusting and out-of-sequence movement along internal structures as a means to maintain a critical taper. This "steady-state model" (Seeber and Gornitz, 1983) suggests that contraction along Himalayan faults progresses at the regional scale toward the foreland, but the hinterland continues to internally thicken. Thus, we propose that subsequent to activity along the Indus-Tsangpo suture during the Late Cretaceous, the Main Central Thrust initiated during the early Miocene as a low-angle thrust (as low as ~7°) that accommodated ~100 km of displacement (see Harrison et al., 1998). In this scenario, the High Himalayan leucogranites were generated due to melting of the kyanite-grade unit of Greater Himalayan Crystallines due to slip along the Main Himalayan Thrust, which provided a small but important amount of heat via a shear stress of ~30 MPa (Harrison et al., 1998, 1999). When the Main Boundary Thrust became active during the late Miocene to Pliocene, the Main Central Thrust was deformed to a steeper angle (30°; Harrison et al., 1998). During the Pliocene to present times, the Main Central Thrust, Main Boundary Thrust, Main Frontal Thrust, and Main Himalayan Thrust have all been active structures.

To test these models of Himalayan convergence, monazites [$(Ce, La, Th)PO_4$] were dated in rocks collected within the Main Central Thrust shear zone along the Bhagirathi River in NW India (Figs. 3 and 4). The Main Central Thrust shear zone in this area is a well-exposed sequence of metamorphic rocks, bounded by the Greater Himalayan Crystallines–Lesser Himalayan Formations contact at its upper level (the Vakrita Thrust, the local Main Central Thrust equivalent) and the Munsiari Thrust at its base (see also Pêcher and Scaillet, 1989; Metcalfe, 1993; Searle et al., 1999). The "in-sequence" model predicts that monazite beneath the Main Central Thrust will record ages consistent with early Miocene movement, whereas the "steady-state model" predicts that post–early Miocene ages are present within the Lesser Himalayan Formations, as these rocks are subjected to increases in pressure and temperature (*P-T*) and fluids, thus triggering chemical reactions and subsequent monazite growth due to movement within the shear zone.

Monazite Paragenesis

Himalayan pelites and granitoids commonly contain monazite as an accessory phase. Monazite is a useful U-Th-Pb geochronometer (see reviews of Parrish, 1990; Harrison et al., 2002) because it (1) incorporates significant amounts of U and Th (Overstreet, 1967) while excluding Pb during crystallization, (2) sustains little radiation damage (e.g., Meldrum et al., 1998), and (3) is resistant to diffusive Pb loss, even at high crustal temperatures (e.g., Cherniak et al., 2004). Inclusions of monazite in

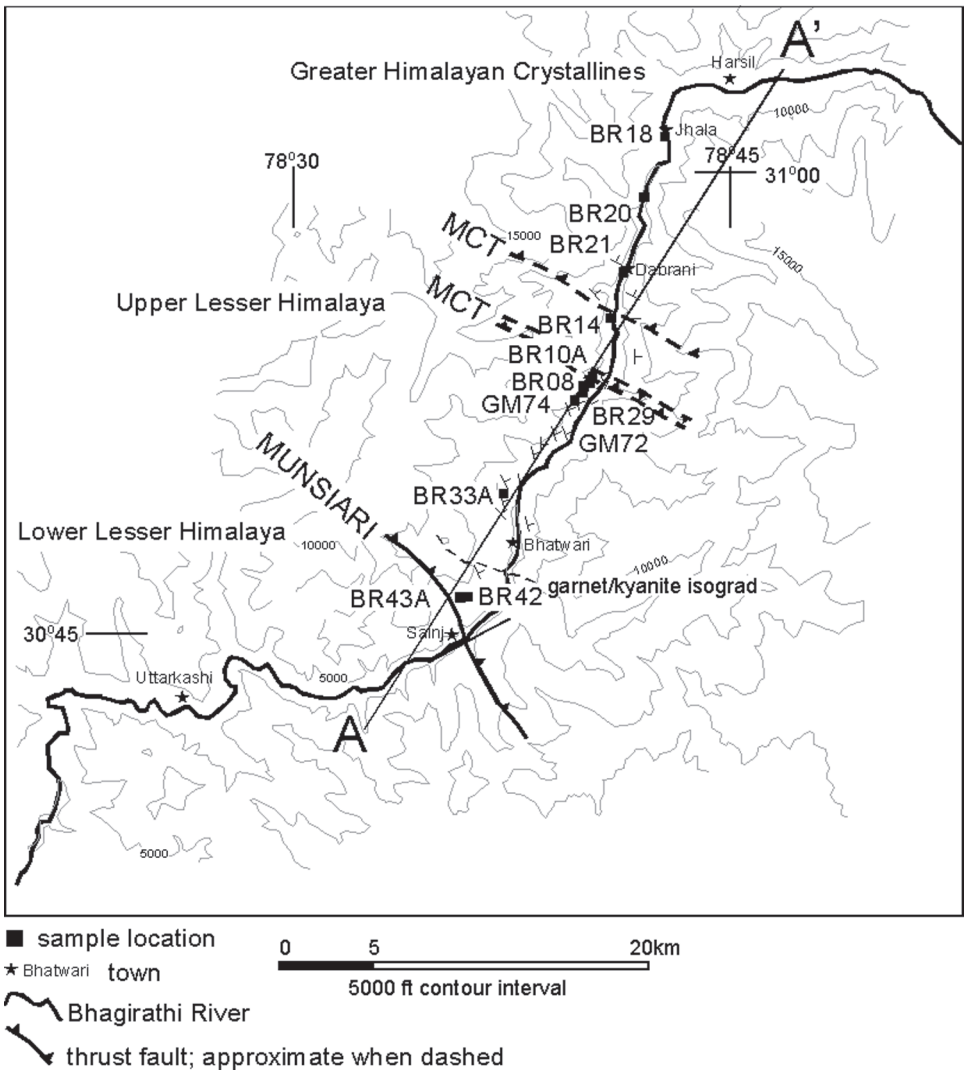

Figure 3. Sample location map of the transect taken along the Bhagirathi River. See Tables 1 and 2 for monazite ages; GM samples were collected by Metcalfe (1993). GM74 contains monazites that average 5.9 ± 0.2 Ma (Catlos et al., 2002b). See Figure 1 for the location of this area relative to the Himalayas and Figure 4 for a cross section along A–A′. MCT—Main Central Thrust.

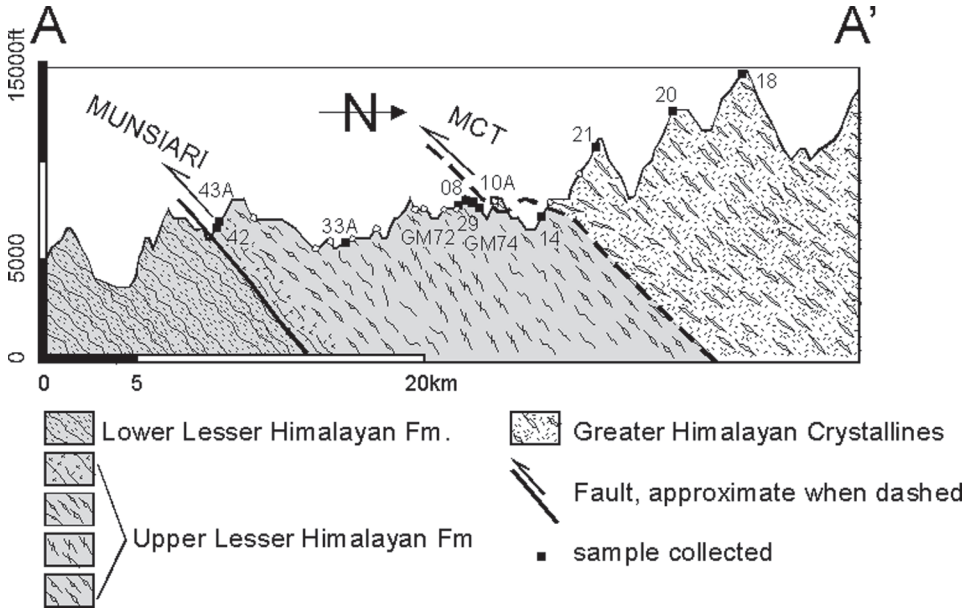

Figure 4. Cross section of the Bhagirathi River transect; for line of section, see Figure 3. All samples are referred to as BR# in the text, except samples GM72 and GM74, which were collected by Metcalfe (1993).

garnet appear armored against dissolution/reprecipitation (e.g., Montel et al., 2000; Catlos et al., 2001). Garnet-bearing assemblages allow peak *P-T* conditions to be determined. When combined with monazite ages, the data are a powerful means with which to ascertain the evolution of metamorphic terranes (e.g., Foster et al., 2000; Catlos et al., 2001; Gilley et al., 2003; Kohn et al., 2004, 2005).

Monazite appears in metapelites in the garnet or staurolite zones (e.g., Smith and Barreiro, 1990; Kingsbury et al., 1993; Catlos et al., 2001; Wing et al., 2003; Kohn and Malloy, 2004; Kohn et al., 2004, 2005), but regional metamorphic (i.e., non-hydrothermal or alteration) monazite has been documented over a large range of temperatures from <400 °C to ~700 °C (Smith and Barreiro, 1990; Kingsbury et al., 1993; Franz et al., 1996; Pyle and Spear, 1999; Ferry, 2000; Townsend et al., 2001; Catlos et al., 2001; Pyle et al., 2001; Wing et al., 2003; Kohn and Malloy, 2004; Kohn et al., 2004, 2005). Some of this range reflects different prograde and retrograde reactions that produce or consume monazite (see review by Catlos et al., 2002a), including the participation of other LREE (light rare earth element) accessory minerals such as allanite, or dissolution/reprecipitation of monazite in response to major silicate reactions (e.g., Pyle and Spear, 2003).

In central Nepal, a rock from the lowermost structural levels of the Main Central Thrust shear zone contains matrix monazite grains as young as 3.3 ± 0.1 Ma (1σ) (Catlos et al., 2001) and 3.0 ± 0.2 Ma (1σ) (Kohn et al., 2004), providing support for the "steady-state model." However, because the Main Central Thrust extends over ~2400 km along strike (Fig. 1), the possibility exists that this event was localized to central Nepal (Stephenson et al., 2001; Searle and Godin, 2003). In addition, the location of the young monazites within lower levels of the Main Central Thrust shear zone has led to speculation that their presence may be related to slip along thrusts associated with the Main Boundary Thrust (Robinson et al., 2003). The Bhagirathi River transect (Fig. 3), located ~800 km west of central Nepal, is an ideal locale to examine the age distribution of monazite exposed within the Main Central Thrust footwall to address these concerns.

METHODS

Samples were collected along an ~50 km stretch of road that parallels the Bhagirathi River north of the town of Uttarkashi (Fig. 3). Monazite was dated in rock thin section using the in situ Th-Pb ion microprobe technique (Harrison et al., 1997; Catlos et al., 2001, 2002a). This approach involves cutting the monazite and region of interest out of the thin section with a high-precision saw and mounting the chip in epoxy with a block of monazite age standards. The method is ideal for petrologic investigations because the ion microprobe is nondestructive of the grain and its textural relationships. Analysis of small grains (~10 μm) and zones within larger grains is feasible, and results are available within a few minutes. Monazite grains were first identified in rock thin section using the Oklahoma State University JEOL 733 electron microprobe. Most of the monazite grains dated here are ~20–200 μm in length and are chemically zoned. Several studies document that chemical zones in monazite can be linked petrologically to a rock's reaction history and *P-T* evolution (Spear

and Pyle, 2002; Kohn et al., 2004; Pyle et al., 2005). Monazite composition may vary because of several factors, including crystal orientation, the transfer of elements from the breakdown of rare earth element (REE)–rich phases under changing *P-T* conditions, competitive crystallization among other REE phases in the rock, or replacement or recrystallization of an original grain during metamorphism (e.g., Cressey et al., 1999; Pyle and Spear, 1999; Zhu and O'Nions, 1999; Townsend et al., 2001; Catlos et al., 2002a; Kohn et al., 2004, 2005). Attempts were made to date specific chemical zones within the monazite as seen in BSE (backscattered electron) images; however, the small grain size with respect to the diameter of the ion microprobe beam precluded significant interpretations in most cases.

After documentation, the region of the thin section that contains the monazite was cut out and mounted in epoxy with about five grains of monazite 554 age standards (Force, 1997), which have been dated at 45 ± 1 Ma by isotope dilution (Harrison et al., 1999). An ion microprobe oxygen beam with an ~30 µm diameter sputtered isotopes of Th and Pb from individual monazite grains. An aperture was used constrict the oval beam to a square shape. This is an important part of in situ analyses, as it minimizes contamination from common Pb possibly found in adjacent grains and grain boundaries. Several spots are analyzed on monazite 554 grains, which are observed to fall along a line in ThO_2^+/Th^+ versus $^{208}Pb^+/Th^+$ space as the analysis sessions progress (see Harrison et al., 1995; Catlos et al., 2002a, for examples). The precision of the ages is primarily limited by the reproduction of this calibration curve, which in this study had a regression (r^2) value of 0.994, a slope of 0.115 ± 0.007 (1σ) and a ThO_2^+/Th^+ intercept of 1.240 ± 0.143 (1σ).

Tables 1 and 2 report the monazite ages; the uncertainty for all ages reported here is ±1σ. In this study, the Eocene to early Miocene monazites yield results with approximately ±3% uncertainty, and the Proterozoic monazites are ±4% (see Tables 1 and 2). The late Miocene to Pliocene ages are the most uncertain, yielding an average ±18%. This may be attributed to (1) ThO_2^+/Th^+ values that did not lie within the range defined by the calibration curve or (2) lower amounts of radiogenic ^{208}Pb ($^{208}Pb^*$). For example, the Eocene to early Miocene and Proterozoic monazites were the most radiogenic (90.1 ± 0.9% and 99.7 ± 0.04% $^{208}Pb^*$ respectively), but the late Miocene to Pliocene averaged only 44.8 ± 6.2% $^{208}Pb^*$. The common Pb correction is a significant factor influencing the precision of ages of monazite grains that contain low amounts of $^{208}Pb^*$.

X-ray maps of Mn, Ca, Fe, and Mg were taken of a garnet in sample BR14 using the energy-dispersive spectrometry (EDS) capability of the Oklahoma State University electron microprobe. A current of 30 nA, beam size of ~1 µm, and count times of 30–35 ms produced the clearest X-ray element maps. Peak *P-T* conditions recorded by sample BR14 were estimated from mineral compositions via garnet-biotite thermometry (Ferry and Spear, 1978; Berman, 1990) and garnet-plagioclase-biotite-muscovite barometry (Hoisch, 1990) using the program GTB: GeoThermoBarometry (Spear and Kohn, 2001). Other calibrations change the *P-T* conditions by ±25 °C and ±50 MPa, which are within uncertainty of the

TABLE 1. GREATER HIMALAYAN CRYSTALLINES MONAZITE AGES (BHAGIRATHI RIVER)

Grain-spot†	Location‡	Th-Pb age (±1σ) (Ma)	ThO_2^+/Th^+ (±1σ)§	$^{208}Pb^*$ (±1σ) (%)#	$^{208}Pb^+/Th^+$ (× 10^3)††
Sample BR18 (31°1.121′N, 78°2.810′E)‡‡					
2-1	M	23.2 (0.6)	3.111 (0.018)	86.6 (1.0)	1.150 (0.027)
1-1	M	20.6 (0.9)	2.959 (0.035)	69.7 (2.3)	1.017 (0.046)
3-1	M	19.5 (0.3)	3.855 (0.027)	89.6 (0.9)	0.965 (0.016)
Sample BR20 (30°59.360′N, 78°41.979′E)					
8-1	M	38.0 (0.8)	3.048 (0.024)	96.8 (0.2)	1.880 (0.039)
7-1	M	37.9 (0.9)	2.944 (0.014)	95.4 (0.3)	1.879 (0.044)
8-2	M	34.3 (0.8)	2.949 (0.015)	96.9 (0.2)	1.698 (0.041)
6-1	M	28.5 (0.6)	3.080 (0.015)	91.0 (0.5)	1.410 (0.028)
6-2	M	23.7 (0.6)	3.249 (0.030)	76.0 (1.5)	1.171 (0.030)
Sample BR21 (30°56.766′N, 78°41.323′E)					
1-1	I	21.1 (0.5)	4.474 (0.014)	93.4 (1.0)	1.044 (0.025)
Sample BR10A (30°53.215′N, 78°40.391′E)					
2-3	M	24.2 (1.2)	2.531 (0.015)	92.9 (0.9)	1.198 (0.061)
1-1	M	24.0 (0.5)	2.993 (0.013)	93.0 (0.6)	1.186 (0.026)
2-1	M	23.6 (0.3)	3.417 (0.017)	93.5 (0.5)	1.167 (0.014)
2-2	M	22.4 (0.3)	3.262 (0.010)	93.8 (0.5)	1.108 (0.014)

†Nomenclature indicates the grain and spot, respectively, of the analyzed monazite. See Figure 5 for BSE images of the grains.
‡Monazite inclusion in garnet is designated as "I", whereas "M" indicates a matrix grain.
§Measured ratio in sample. Ideally, the ThO_2^+/Th^+ lies within the range defined by the standard monazite.
#Percent radiogenically derived ^{208}Pb.
††Corrected sample ratio assuming $^{208}Pb/^{204}Pb = 39.5 \pm 0.1$ (Stacey and Kramers, 1975).
‡‡Sample name and GPS location (see also Figs. 3 and 4).

TABLE 2. BHAGIRATHI RIVER TRANSECT, LESSER HIMALAYAN MONAZITE AGES

Grain-spot†	Location‡	Th-Pb age (±1σ) (Ma)	ThO_2^+/Th^+ (±1σ)§	$^{208}Pb^*$ (±1σ) (%)#	$^{208}Pb^+/Th^+$ (× 10^3)††
Sample BR14 (30°55.280′N, 78°41.140′E)‡‡					
9-1	M	6.5 (1.4)	3.930 (0.035)	32.9 (6.7)	0.324 (0.067)
8-1	M	5.4 (1.8)	5.796 (0.051)	27.6 (9.3)	0.265 (0.090)
4-1	M	4.5 (1.3)	3.277 (0.028)	21.2 (6.0)	0.222 (0.063)
3-1	M	4.4 (0.7)	3.910 (0.042)	54.7 (9.1)	0.217 (0.037)
1-1	M	4.2 (0.8)	3.457 (0.038)	29.9 (5.9)	0.208 (0.041)
2-1	M	3.8 (0.5)	3.446 (0.030)	39.8 (5.2)	0.190 (0.025)
2-2	M	3.6 (0.9)	3.160 (0.022)	35.8 (8.4)	0.180 (0.042)
7-1	M	3.6 (0.8)	4.097 (0.021)	35.9 (7.5)	0.179 (0.038)
Sample BR29 (30°52.996′N, 78°39.990′E)					
1-1	M	1532 (12)	3.435 (0.008)	99.9 (0.01)	78.72 (0.637)
1-2	M	43.7 (2.3)	3.049 (0.005)	93.1 (0.6)	2.163 (0.113)
1-4	M	9.9 (0.6)	2.694 (0.004)	68.9 (1.8)	0.488 (0.029)
1-3	M	8.4 (0.3)	3.151 (0.007)	57.3 (1.5)	0.416 (0.013)
1b-1	M	4.8 (0.2)	3.258 (0.010)	69.8 (3.2)	0.239 (0.012)
4-2	M	4.3 (0.1)	3.688 (0.009)	79.7 (2.3)	0.213 (0.007)
5-2	M	4.2 (0.1)	3.542 (0.015)	81.2 (2.4)	0.208 (0.007)
4-1	M	4.1 (0.2)	3.763 (0.008)	73.8 (3.0)	0.205 (0.009)
5-1	M	4.1 (0.1)	3.655 (0.006)	75.2 (2.6)	0.201 (0.007)
Sample BR08 (30°53.427′N, 78°40.352′E)					
1-1	M	2318 (276)	2.004 (0.030)	99.9 (0.01)	121.5 (15.32)
Sample BR33A (30°49.779′N, 78°37.448′E)					
6-1	M	1697 (13)	3.439 (0.012)	99.9 (0.01)	87.61 (0.72)
5-1	M	1472 (39)	2.848 (0.011)	99.9 (0.01)	75.52 (2.05)
4-1	M	1341 (13)	3.333 (0.010)	99.9 (0.01)	68.61 (0.67)
Sample BR42 (30°46.235′N, 78°35.849′E)					
1-1	M	443 (31)	2.312 (0.014)	98.4 (0.1)	22.14 (1.58)
2-1	M	8.7 (1.0)	2.870 (0.008)	24.8 (2.8)	0.430 (0.051)
4-1	M	2.6 (0.7)	3.260 (0.011)	16.2 (4.1)	0.131 (0.034)
Sample BR43A (30°46.235′N, 78°35.849′E)					
1-1	M	1.0 (0.5)	2.936 (0.036)	18.1 (9.9)	0.049 (0.027)
2-1	M	0.8 (0.2)	2.561 (0.011)	29.7 (9.0)	0.038 (0.012)

†Nomenclature indicates the grain and spot, respectively, of the analyzed monazite. See Figures 7, 9, 10, and 11 for BSE images of the grains.
‡"M" indicates a matrix grain.
§Measured ratio in sample. Ideally, the ThO_2^+/Th^+ lies within the range defined by the standard monazite.
#Percent radiogenically derived ^{208}Pb.
††Corrected sample ratio assuming $^{208}Pb/^{204}Pb = 39.5 \pm 0.1$ (Stacey and Kramers, 1975).
‡‡Sample name and GPS location (see also Figs. 3 and 4).

result. The compositions of garnet at the lowest spessartine and lowest Fe/(Fe + Mg) values and matrix muscovite, plagioclase, and biotite were quantitatively obtained using the electron microprobe operating at an accelerating potential of 20 kV and a probe current of ~25 nA (Table 3). Plagioclase grains have an anorthosite content of 25 ± 2%. *P-T* conditions were determined for each composition in Table 3 and averaged. For compositional analyses, maximum count times were 20 s for each spot, and raw data were reduced using the PAP matrix correction.

RESULTS

Greater Himalayan Crystallines

Samples BR10A, BR18, BR20, and BR21 were collected from the Greater Himalayan Crystallines (Figs. 3 and 4; Table 1), a unit of garnet-bearing gneisses. Sample BR10A is classified as a Greater Himalayan rock based on lithology, field observations (see also Pêcher and Scaillet, 1989; Metcalfe, 1993), and monazite ages (average = 23.6 ± 0.7 Ma). These samples all contain rounded or flattened garnet + biotite + muscovite + plagioclase + chlorite + zircon + monazite + quartz + ilmenite (Fig. 5). Monazites in these rocks range from Eocene (38.0 ± 0.8 Ma; sample BR20) to Miocene (19.5 ± 0.3 Ma; sample BR18). The Eocene-Oligocene ages are consistent with a phase of Barrovian metamorphism of the Greater Himalayan Crystallines termed the Eohimalayan Event (e.g., Metcalfe, 1993; Hodges et al., 1996; Le Fort, 1996; Wiesmayr and Grasemann, 2002). The Miocene ages can be correlated to timing movement within the Main Central Thrust slip in a broad sense (e.g., Schelling and Arita, 1991; Vannay and Steck, 1995; Hodges et al., 1996; Stephenson et al., 2001).

TABLE 3. MINERAL COMPOSITIONS USED TO GENERATE BR14 *P-T* CONDITIONS

	Garnet	Garnet	Biotite	Plagioclase	Plagioclase	Muscovite
SiO_2	37.5	37.6	41.1	62.9	64.0	48.7
Al_2O_3	20.3	20.3	27.5	23.1	22.8	33.9
MnO	0.49	0.91	0.08	<0.01	0.03	0.02
MgO	1.67	1.76	4.53	0.01	0.01	0.78
CaO	3.12	2.86	<0.01	4.84	4.35	0.01
Na_2O	<0.01	0.01	0.86	8.33	8.66	1.31
FeO	36.9	36.1	12.5	0.06	0.01	1.28
TiO_2	0.02	0.13	1.09	<0.01	<0.01	0.29
Cr_2O_3	0.04	<0.01	<0.01	<0.01	0.06	0.02
K_2O	nm	nm	8.20	0.07	0.08	8.86
Total	100.0	99.8	95.8	99.2	100.0	95.2
Si	3.04	3.05	5.80	2.80	2.82	6.42
Al	1.94	1.94	4.58	1.21	1.19	5.26
Mn	0.03	0.06	0.01	<0.01	<0.01	0.00
Mg	0.20	0.21	0.95	<0.01	<0.01	0.15
Ca	0.27	0.25	<0.01	0.23	0.21	0.00
Na	<0.01	<0.01	0.24	0.72	0.74	0.33
Fe	2.50	2.45	1.47	<0.01	<0.01	0.14
Ti	<0.01	0.01	0.12	<0.01	<0.01	0.03
Cr	<0.01	<0.01	<0.01	<0.01	<0.01	<0.01
K	nm	nm	1.48	<0.01	<0.01	1.49
Total	8.0	8.0	14.6	5.0	5.0	13.8

Note: The oxides are reported in weight percent, whereas the cations are reported as atoms per formula unit. Garnet analyses were taken at the lowest Mn and Fe/Fe + Mg values. Matrix plagioclase, biotite, and muscovite analyses were taken in close proximity to garnet. Two plagioclase analyses of differing Ca content were used in the thermobarometric calculations. nm—not measured.

Along the Bhagirathi River transect, a "late brittle structure" (termed the Jhala fault) has been reported to separate quartzofeldspathic sillimanite-grade gneisses from metasediments with bands of K-feldspar augen gneisses near the town of Jhala (Metcalfe, 1993; Searle et al., 1999). However, no change in structure or lithology is observed near the town of Jhala (Fig. 6), which is surrounded by homoclinally north-dipping garnet-bearing gneisses. Although the fault has been mapped within the sillimanite zone, rocks sampled across the supposed structure only reached kyanite-grade *P-T* conditions (e.g., 600 ± 40 °C and 8.5 ± 1.2 kbar to the north, and 600 ± 40 °C and 8.9 ± 1.3 kbar to the south) (Metcalfe, 1993). In addition, these rocks yield similar Oligocene-Miocene mica ages (20.8 ± 0.6 Ma to the north and 21.1 ± 0.6 Ma to the south) (Metcalfe, 1993). Sample BR18 was collected near the town of Jhala (Fig. 6) and contains monazites that are similar in age to those at structurally lower levels.

Lesser Himalayan Formations

Monazites dated in the Lesser Himalayan Formations were only found in the matrix of the rock (Table 2). Matrix monazite grains present unique problems in the interpretation of their ages because they can be subjected to reactions during retrogression and/or subsequent metamorphism (e.g., Catlos et al., 2002a). Several studies document partial melting reactions that dissolve earlier-formed monazite and subsequent melt crystallization that reforms it (e.g., Pyle and Spear, 1999, 2003; Kohn et al., 2004, 2005). Thus, a high-temperature rock may have different generations of monazite that formed at lower temperature (the original "monazite-in"), and others that reflect later reactions at higher temperature. Lower-temperature alteration can also cause monazite dissolution/reprecipitation. This has been documented both in contact metamorphic settings (e.g., Townsend et al., 2001) and in late-stage fractures in high-grade metamorphic rocks (e.g., Kohn et al., 2004, 2005). However, as explained below, the textural relationships of the monazite being dated can help evaluate the presence of these reactions. In addition, the ability to date multiple grains in a single sample can evaluate for the presence of these potentially fluid-mediated reactions in terms of heterogeneous age distributions.

Samples BR14 and BR29 were collected from the footwall of the Main Central Thrust, less than 1 km beneath the Greater Himalayan Crystallines (Figs. 3 and 4). Figure 7 shows BSE images of monazites found in BR14, which has euhedral garnets and ilmenite inclusions that extend into the matrix. Matrix monazites are aligned with the overall fabric of the rock defined the chlorite, biotite, and ilmenite grains (Fig. 7). Eight BR14 matrix monazites yield an average age of 4.5 ± 1.1 Ma with a Mean Square Weighted Deviation (MSWD) of 0.8, consistent with a single population (Table 2).

X-ray element maps and a compositional traverse show that the garnet preserves prograde zoning and experienced minimal diffusional modification or retrogression (Fig. 8). The *P-T* conditions recorded by sample BR14 are 540 ± 25 °C and

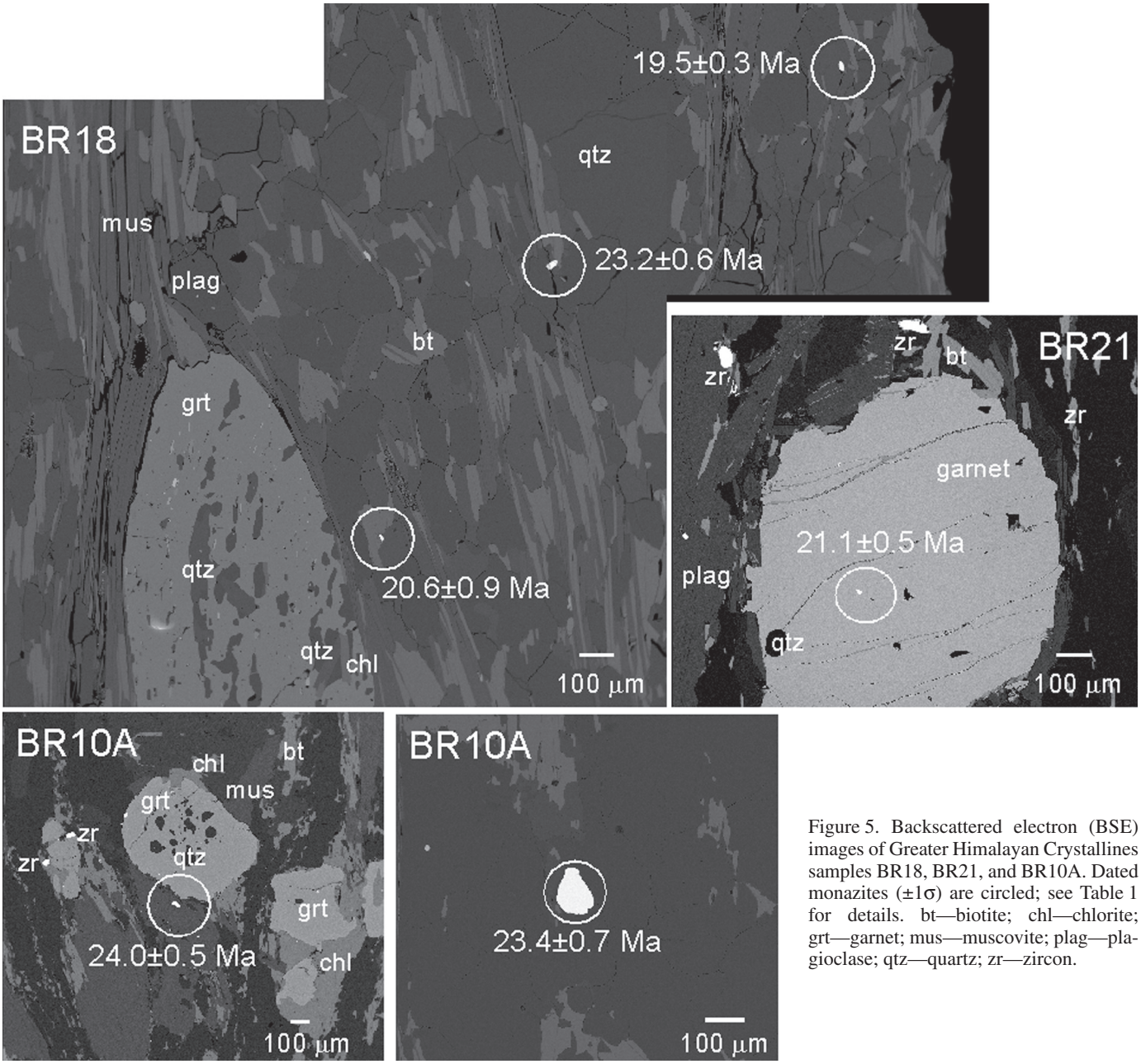

Figure 5. Backscattered electron (BSE) images of Greater Himalayan Crystallines samples BR18, BR21, and BR10A. Dated monazites (±1σ) are circled; see Table 1 for details. bt—biotite; chl—chlorite; grt—garnet; mus—muscovite; plag—plagioclase; qtz—quartz; zr—zircon.

700 ± 180 MPa (Table 3). These estimates are consistent with the sample's mineral assemblage, prograde garnet X-ray element maps (Fig. 8), and the *P-T* conditions of rocks collected nearby (see Metcalfe, 1993). If we assume that these monazites formed under a geobaric gradient of 0.035 km/MPa and followed the presently dipping 48°NE ramp observed in the field, this rock exhumed at a rapid rate of ~7 mm/yr [(0.035 km/MPa × 700 MPa) / (4.5 m.y. × sin 48°)]. Although this rate is highly uncertain due to the difficulty in estimating the parameters necessary in this calculation, the minimum exhumation rate (vertical) is 4.5 mm/yr because of the calculated depth with age. The presence of such young monazite ages in a high-grade metamorphic rock located directly beneath the Main Central Thrust indicates the structure must have been active at this time.

Sample BR29 (collected at similar structural levels as sample BR14) contains three ~100 μm long monazite grains that yield 4.8 ± 0.2 Ma to 4.1 ± 0.1 Ma (Table 2; Fig. 9). The Pliocene grains are found adjacent to or as inclusions within large biotite grains that parallel the overall foliation of the sample. BR29 also contains a large ~500 μm long monazite inclusion in biotite that appears sector-zoned in BSE and has a 1532 ± 12 Ma core. Several workers report the presence of Early to Middle Proterozoic ages within the Lesser Himalayan Formations (e.g., Ahmad et al., 1999; Miller et al., 2000; Sarkar et al., 2000; Catlos et al.,

Figure 6. Field shot of the homoclinally dipping Greater Himalayan Crystallines exposed near the town of Jhala. The location of sample BR18 is indicated with average monazite age (±1σ).

2002b) and suggest the ages reflect tectonic or magmatic events related to or older than the assembly of India. Several structurally lower samples contain Early to Middle Proterozoic monazites (BR08, BR33A; Fig. 10), indicating that monazite was present in the Lesser Himalayan Formations prior to Indo-Asia collision. These older monazite grains may have been the reactant material for subsequent monazite precipitation during the Pliocene.

The BR29 grain has a core that appears darker than its outer rim in BSE, and contains bright ~1 μm inclusions of thorite (Fig. 9). In this case, the ion microprobe could be positioned to avoid the thorite inclusions and analyze brighter and darker regions of the grain. Two spots on the darker region yield ages of 1532 ± 12 Ma and 43.7 ± 2.3 Ma, indicating that the Th-Pb isotopic systematics of monazite may not be reflected by its whole-mineral chemistry as revealed by BSE. The chemical composition of this monazite grain, which is qualitatively indicated as changes in brightness in the BSE image, may be primarily controlled by its crystal orientation (e.g., Cressey et al., 1999) or other factors (see Catlos et al., 2002a). Ages of the grain that range from 43.7 ± 2.3 Ma to 8.4 ± 0.3 Ma (Table 2; Fig. 9) may not be significant tectonically, instead representing mixing of the older ca. 1532 Ma core and younger ca. 4 Ma event.

The presence of the Pliocene monazite grains in sample BR29 lends support for the hypothesis that a tectonic event occurred in the footwall of the Main Central Thrust during this time, as suggested by the monazites dated in sample BR14. In addition, Catlos et al. (2002b) report 5.9 ± 0.2 Ma (MSWD = 0.4) ages of matrix monazite grains collected near sample BR29 (sample GM74; Figs. 3 and 4), which also provide support for late Miocene–Pliocene Main Central Thrust activity directly

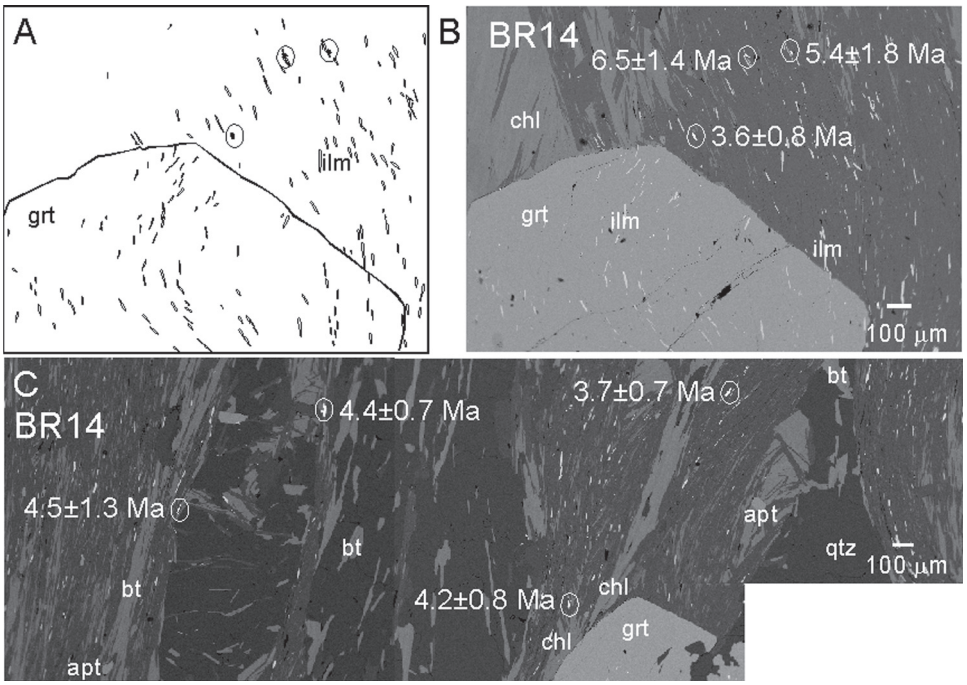

Figure 7. (A) Cartoon of sample BR14 euhedral garnet, ilmenite grains, and monazite (circled). See Figure 8 for X-ray element maps and a compositional transect across this garnet. (B) BSE image of the same region; monazite ages are ±1σ. (C) BSE image of another region of sample BR14, with monazite ages indicated. See Table 2 for analysis details. apt—apatite; bt—biotite; chl—chlorite; grt—garnet; ilm—ilmenite; qtz—quartz.

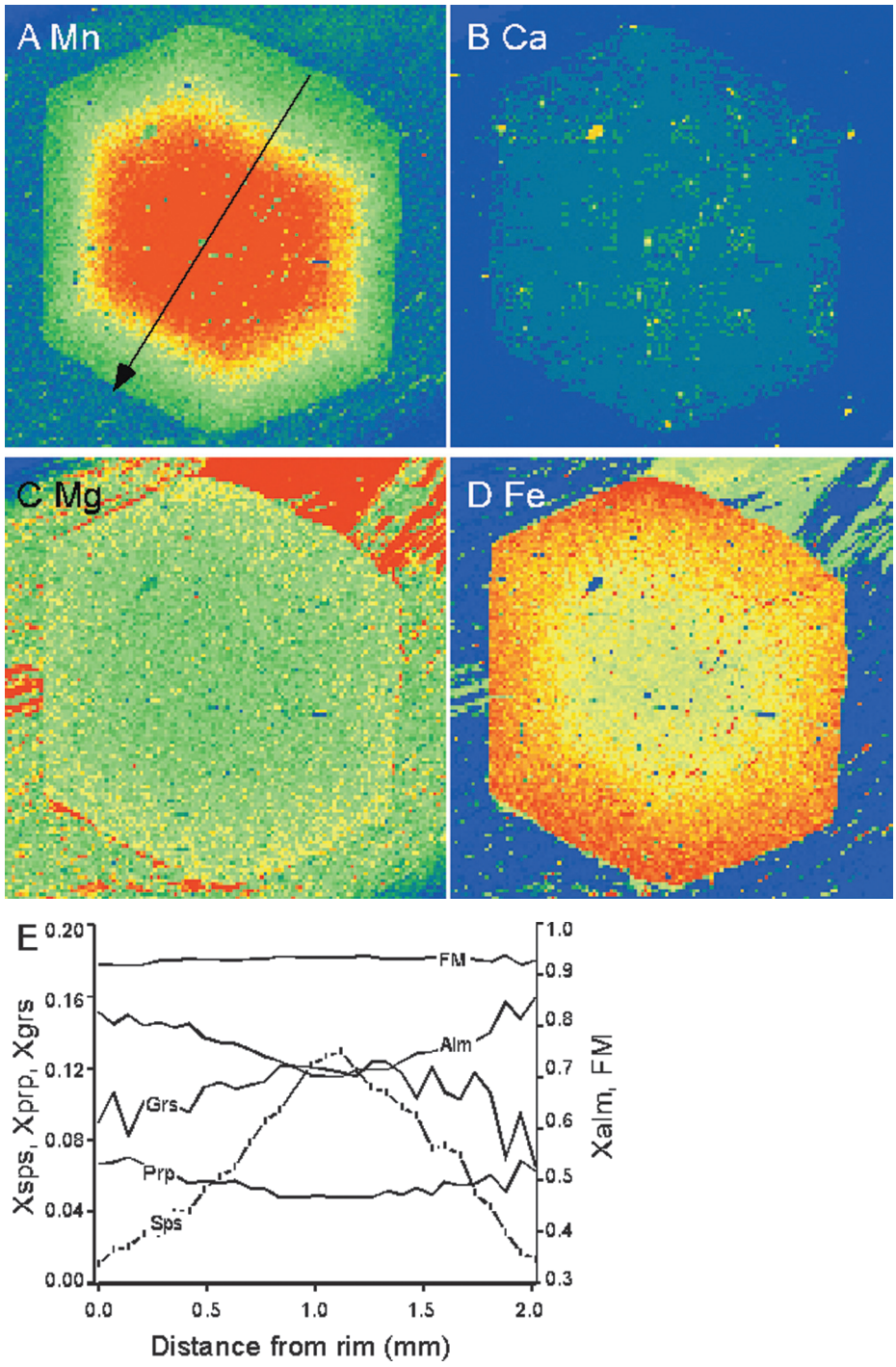

Figure 8. X-ray element maps of the BR14 garnet in Mn (A), Ca (B), Mg (C), and Fe (D). The arrow shows the location of the compositional traverse (E) from rim to rim of the BR14 garnet. FM—Fe/(Fe + Mg); Alm—almandine; Grs—grossular; Prp—pyrope; Sps—spessartine; X—mole fraction. Tick marks on the spessartine profile show the position of each analysis.

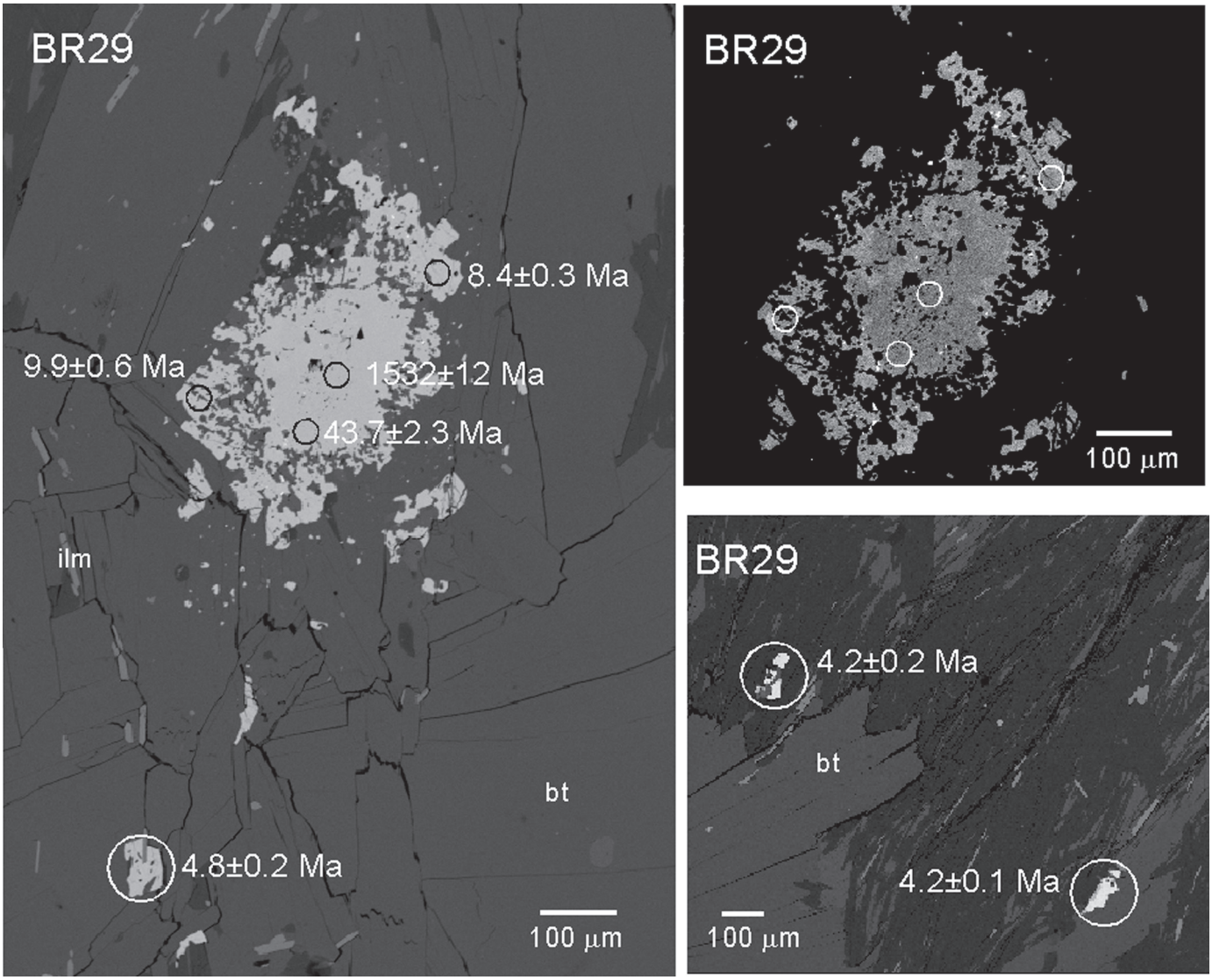

Figure 9. BSE images of monazites in Lesser Himalayan sample BR29. Dated monazites (±1σ) are circled; see Table 2 for details.

beneath the structure in this area. Although this rock did not contain garnet, a sample close by yields 500 ± 40 °C and 700 ± 200 MPa (sample GM72; Metcalfe, 1993), within uncertainty of the *P-T* conditions of sample BR14.

Samples BR42 and BR43A were collected from the base of the Main Central Thrust shear zone within the Munsiari Thrust (Figs. 3, 4, and 11). These rocks contain chlorite + muscovite + monazite + iron oxides and appear to be hydrothermally produced or altered. BR42 contains monazites that range in age from 443 ± 31 Ma to 2.6 ± 0.7 Ma. The Ordovician age may represent a monazite grain from a Lesser Himalayan granite (e.g., Valdiya, 1995; Islam et al., 1999) or partial dissolution and subsequent resetting of a Proterozoic monazite. The Pliocene monazite grain in sample BR42, along with monazites in sample BR43A that are 1.0 ± 0.5 Ma and 0.8 ± 0.2 Ma, are the youngest monazites ever reported from the Himalayas. These grains are in close association with iron oxides in a muscovite-rich vein, indicating a hydrothermal origin.

DISCUSSION

The presence of two samples directly beneath the Main Central Thrust in the Bhagirathi River region of NW India that contain matrix monazite grains that are 4.5 ± 1.1 Ma (T = 540 ± 25 °C, P = 700 ± 180 MPa) and 4.3 ± 0.1 Ma (five grains) is categorically indicative of metamorphism within the Main Central Thrust shear zone during the Pliocene. We interpret that a phase of motion occurred along the structure itself during this time. Although the magnitude of displacement is highly uncertain due to the difficulty in estimating the parameters necessary in the

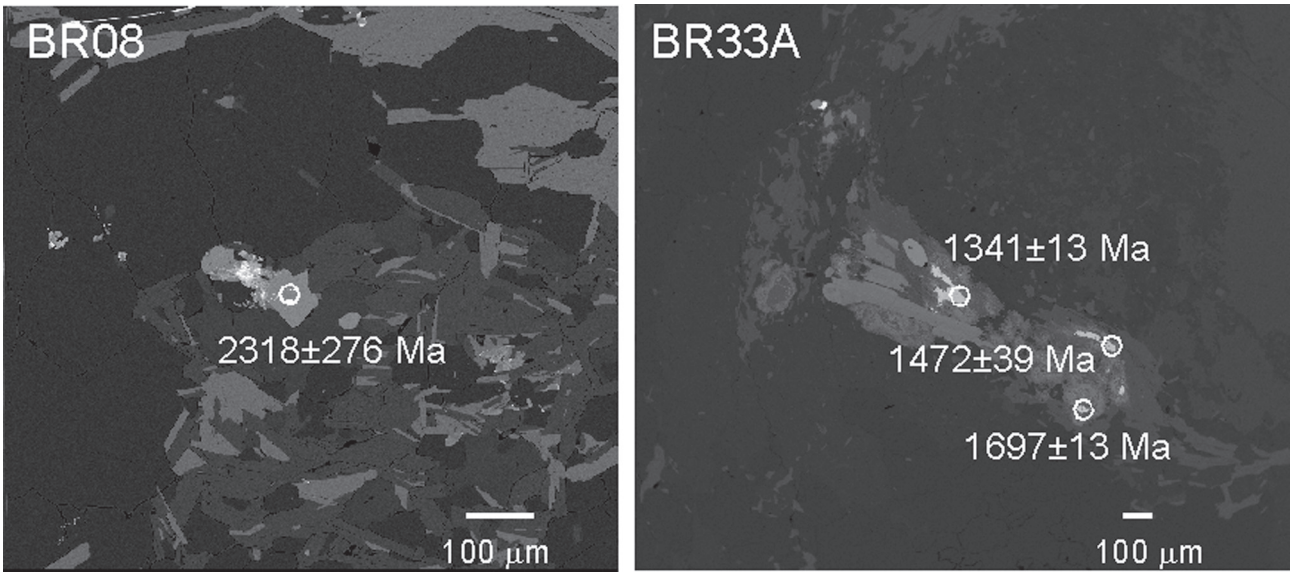

Figure 10. BSE images of monazites in Lesser Himalayan samples BR08 and BR33A. Dated monazites (±1σ) are circled; see Table 2 for details. These monazite grains are located within large allanite grains.

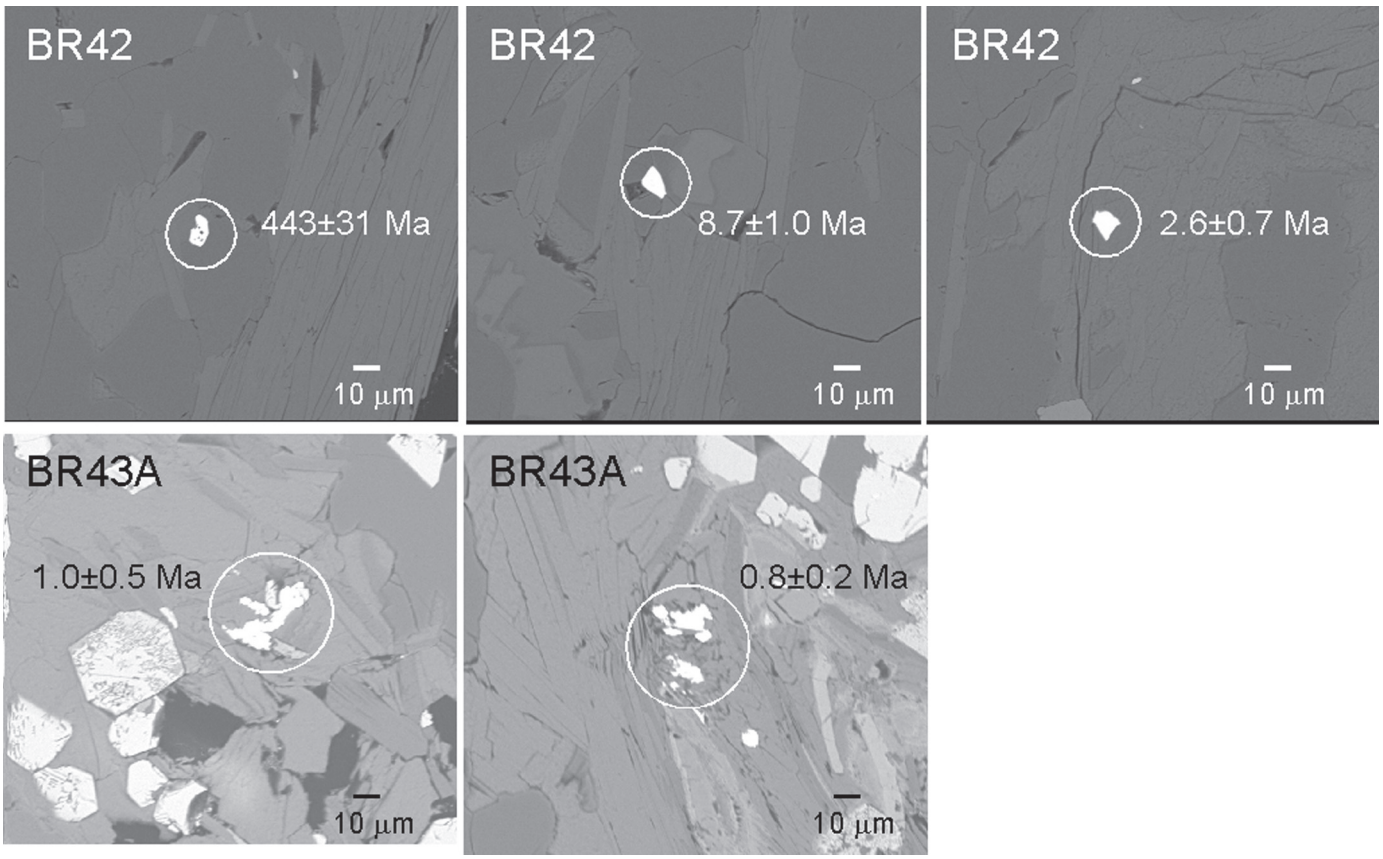

Figure 11. BSE images of monazites in Lesser Himalayan samples BR42 and BR43A. Dated monazites (±1σ) are circled; see Table 2 for details. Minerals in this rock include chlorite, iron oxides, and muscovite.

calculations, this rock may have traveled ~33 km toward the surface since the Pliocene [(0.035 km/MPa × 700 MPa) / sin (48°)]. This magnitude is a significant component (15%–24%) of the overall total displacement estimated for the Main Central Thrust of ~140–210 km from structural studies (see Schelling and Arita, 1991; Srivastava and Mitra, 1994).

These samples that contain the Pliocene monazite grains are located just south of a hanging-wall rock that contains a 21.1 ± 0.5 Ma monazite inclusion in garnet (Fig. 5). The result, in combination with observations of Pliocene monazite ages in central Nepal and late Miocene monazite ages in eastern Nepal (Fig. 12) (Catlos et al., 2001, 2002b; Kohn et al., 2004), indicates that modeling the Himalayas as a region where plate convergence shifts solely toward the foreland is an oversimplification (i.e., the "in-sequence" model). Contraction progressed regionally toward the foreland, but the hinterland continued to thicken internally, as predicted by the "steady-state model" (Seeber and Gornitz, 1983).

In central Nepal, monazite ages show a trend from ca. 20–15 Ma at the Greater Himalaya–Lesser Himalaya Formations contact (= Main Central Thrust sensu stricto), to ca. 7–3 Ma at the base of the shear zone (Fig. 12) (Catlos et al., 2001). The apparent younging of ages from north to south led to the idea that the shear zone can be modeled as the systematic emplacement of thrust sheets within a duplex (Robinson et al., 2003; Kohn et al., 2004). In this model, the Lesser Himalayan Duplex contains stratigraphically, chronologically, and metamorphically distinctive thrust packages below the Greater Himalaya–Lesser Himalaya Formations contact (see DeCelles et al., 1998, 2001, 2002; Robinson et al., 2003; Kohn et al., 2004). Within the duplex, the Ramgahr Thrust and other structures located south of the contact accommodate convergence after the Main Central Thrust ceases movement in the early Miocene. Deformation shifts systematically to these other structurally lower thrusts with movement documented as late as ca. 3 Ma in central Nepal (Catlos et al., 2001; Robinson et al., 2003; Kohn et al., 2004). The amount of convergence accommodated by the Lesser Himalayan Duplex is estimated by field observations as well as geochemical analyses of rocks within each individual thrust, which can be lithologically, chemically, and chronologically mapped (see Kohn et al., 2004). This model is opposed to the idea that the Main Central Thrust shear zone is a broad zone of diffuse deformation that extends for many kilometers above and below the contact.

The distribution of monazite ages within the Lesser Himalayan Formations along the Bhagirathi River suggest that the duplex in NW India, if it exists, developed from ca. 4 to ca. 1 Ma, versus from ca. 15 to ca. 3 Ma in central Nepal. However, this observation is contingent on the ca. 1 Ma monazite grains timing movement within the Munsiari Thrust, and active hydrothermal systems are commonly located within the Main Central Thrust shear zone (e.g., Evans et al., 2001).

In the Everest region of Nepal and the Sikkim region of NE India, Main Central Thrust shear zone monazite grains yield ages as young as 10.3 ± 0.8 Ma and 10.5 ± 0.6 Ma, respectively (Catlos et al., 2002b; Catlos et al., 2004). Searle and Godin (2003) argue that the wide range of ages along and across Main Central Thrust strike is evidence that the structure has not experienced movement since the early Miocene, and instead reflects monazite retrogression, growth over widely differing temperature ranges, and/or inheritance. Although monazite in the matrix of a sample can be affected by subsequent metamorphism and retrogression, many of the ages shown in Figure 12 are from inclusions

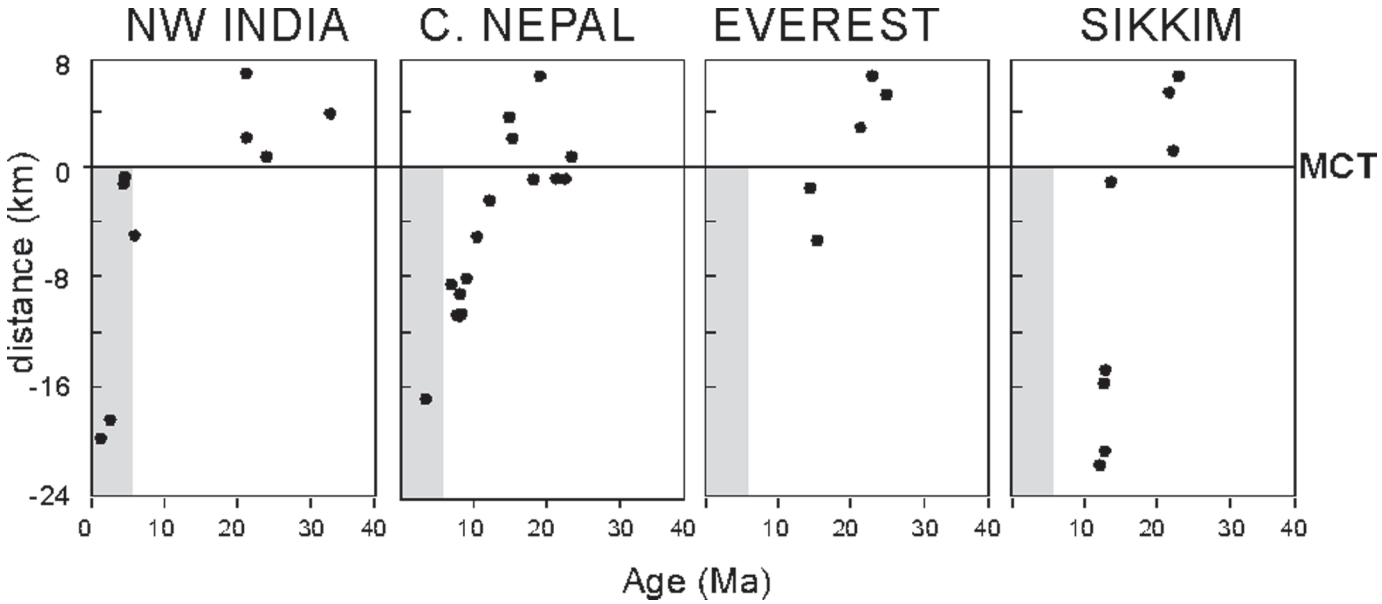

Figure 12. Approximate average monazite ages roughly plotted against structural distance from the Main Central Thrust (MCT) (from Catlos et al., 2001, 2002b, 2004). Shaded area signifies the start of the Pliocene (ca. 5.4 Ma).

in garnet and are consistent with a single population (see Catlos et al., 2001, 2002b, 2004). We argue that the observed distribution of monazite ages is evidence that Main Central Thrust shear zone moved at temporally distinct times along strike.

Because of the striking lateral continuity of Himalayan lithologies (Fig. 1), the widespread presence of Oligocene-Miocene metamorphism recorded by the Greater Himalayan Crystallines (see review by Guillot et al., 1999), as well as the remarkable consistency of emplacement times of the High Himalayan and North Himalayan granites (see review by Harrison et al., 1998, 1999), an expectation arises that processes operating in NW Indian Himalayas should be temporally similar to those occurring in the range in Nepal and NE India. The span of monazite ages across Main Central Thrust strike and lack of Pliocene ages in eastern Nepal and the Sikkim region could reflect changing boundary conditions controlling the mechanics of Indo-Asia collision since the early Miocene. Extrusion along left-lateral strike-slip faults north of the Himalayas (Fig. 13) (e.g., Tapponnier et al., 1982, 2001) may have accommodated convergence and affected the partitioning of strain within the Himalayas, which is reflected in the timing of metamorphism within the Main Central Thrust shear zone.

Main Central Thrust movement during the Pliocene would significantly change the slope of the Himalayas, resulting in a rapid increase of erosion. Evidence for this increase are found in paleosols from a sedimentary section south of the Bhagirathi River transect exposed along the Somb River in Himachal Himalayas. Stable isotopes of carbon, oxygen, and hydrogen and Sr isotopic ratios from this section yielded results consistent with increased weathering and high rainfall at ca. 4 Ma (Ghosh et al., 2004).

The persistence of the Main Central Thrust as a prominent topographic break indicates that the structure continues to play an important role in controlling mass movement and deformation (Hodges et al., 2004). Seismicity in close proximity to the Main Central Thrust in NW India includes the 1999 Chamoli (M_s = 6.6) (Sarkar et al., 2001) and 1991 Uttarkashi earthquakes (m_b = 6.6) (Kayal, 1996) as well as historical magnitude 5–7 earthquakes (Badrinath 1803, Gangotri 1816, Mussoorie 1865) (Oldham, 1883). These earthquakes were located between the Main Central Thrust and the Main Boundary Thrust within a clearly identifiable ~50 km wide zone of predominately moderate ($5 \leq m_b \leq 6$) earthquakes termed the Main Himalayan Seismic Zone (Ni and Barazangi, 1984). Seismic activity in this zone has been linked to the underthrusting of the Lesser Himalayan Formations beneath the Greater Himalayan Crystallines, and supports the hypothesis that the Main Central Thrust shear zone is presently active in NW India (Sarkar et al., 2001; Virk and Walia, 2001).

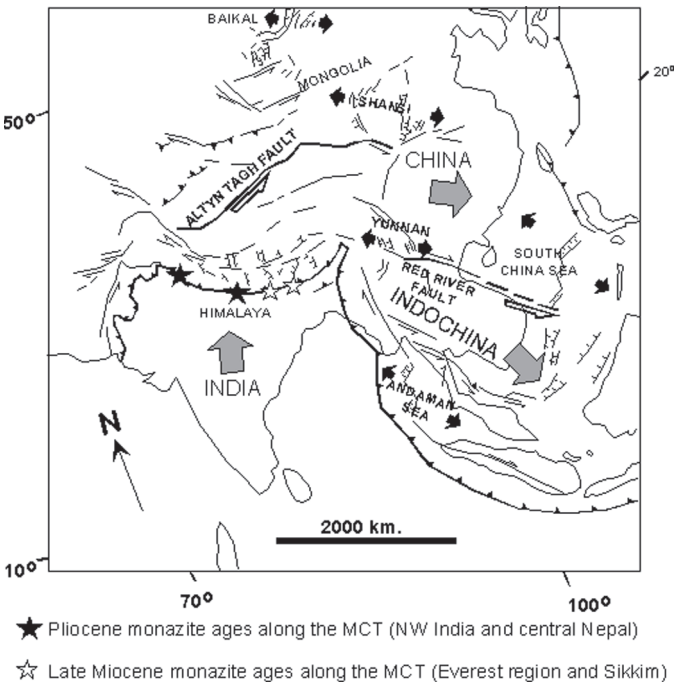

Figure 13. The present-day deformation pattern of Asia (after Tapponnier et al., 1982). Structures thought to have formed and evolved due to the indentation of India include the Altyn Tagh and Red River faults, the South China and Andaman Seas, and the Yunnan and Shansi grabens. The locations where the youngest (Pliocene or late Miocene) monazite ages have been found within the Main Central Thrust shear zone are indicated by stars. MCT—Main Central Thrust.

ACKNOWLEDGMENTS

This work was supported by awards to E.J.C. and R.A.M. from the National Science Foundation (OISE-0217598) and C.S.D. from the Department of Science and Technology of India. We thank the UCLA (University of California, Los Angeles) Ion Microprobe Facility, which is partly supported by a grant from the Instrumentation and Facilities Program, Division of Earth Sciences, National Science Foundation. Samples were collected in the field with assistance from An Yin, A.C. Pandey, and B.K. Sharma. This paper benefited from reviews by Chris Daniel, Peter DeCelles, Matt Kohn, and Kelin Whipple.

REFERENCES CITED

Ahmad, T., Mukherjee, P.K., and Trivedi, J.R., 1999, Geochemistry of Precambrian mafic magmatic rocks of the western Himalaya, India: Petrogenetic and tectonic implications: Chemical Geology, v. 160, p. 103–119, doi: 10.1016/S0009-2541(99)00063-7.

Arita, K., 1983, Origin of the inverted metamorphism of the Lower Himalaya, central Nepal: Tectonophysics, v. 95, p. 43–60, doi: 10.1016/0040-1951(83)90258-5.

Beck, R.A., Burbank, D.W., Sercombe, W.J., Khan, A.M., and Lawrence, R.D., 1996, Late Cretaceous ophiolite obduction and Paleocene India-Asia collision in the westernmost Himalaya: Geodinamica Acta, v. 9, p. 114–144.

Berger, A., Jouanne, F., Hassani, R., and Mugnier, J.L., 2004, Modeling the spatial distribution of present-day deformation in Nepal: How cylindrical is the Main Himalayan Thrust in Nepal?: Geophysical Journal International, v. 156, p. 94–114, doi: 10.1111/j.1365-246X.2004.02038.x.

Berman, R.G., 1990, Mixing properties of Ca-Mg-Fe-Mn garnets: American Mineralogist, v. 75, p. 328–344.

Brozovic, N., and Burbank, D.W., 2000, Dynamic fluvial systems and gravel progradation in the Himalayan foreland: Geological Society of America Bulletin, v. 112, p. 394–412, doi: 10.1130/0016-7606(2000)112<0394:DFSAGP>2.3.CO;2.

Burchfiel, C.B., Zhiliang, C., Hodges, K.V., Yuping, L., Royden, L.H., Changrong, D., and Jiene, X., 1992, The South Tibetan Detachment System, Himalayan orogen: Extension contemporaneous with and parallel to shortening in a collisional mountain belt: U.S. Geological Survey Special Paper 269, p. 1–40.

Burg, J.P., Brunel, M., Gapais, D., Chen, G.M., and Liu, G.H., 1984, Deformation of leucogranites of the crystalline Main Central Sheet in southern Tibet (China): Journal of Structural Geology, v. 6, p. 535–542, doi: 10.1016/0191-8141(84)90063-4.

Catlos, E.J., Harrison, T.M., Kohn, M.J., Grove, M., Ryerson, F.J., Manning, C.E., and Upreti, B.N., 2001, Geochronologic and thermobarometric constraints on the evolution of the Main Central Thrust, central Nepal Himalaya: Journal of Geophysical Research, v. 106, p. 16,177–16,204, doi: 10.1029/2000JB900375.

Catlos, E.J., Gilley, L.D., and Harrison, T.M., 2002a, Interpretation of monazite ages obtained via in situ analysis: Chemical Geology, v. 188, p. 193–215, doi: 10.1016/S0009-2541(02)00099-2.

Catlos, E.J., Harrison, T.M., Manning, C.E., Grove, M., Rai, S.M., Hubbard, M.S., and Upreti, B.N., 2002b, Records of the evolution of the Himalayan orogen from in situ Th-Pb ion microprobe monazite dating: Eastern Nepal and western Garhwal: Journal of Asian Earth Sciences, v. 20, p. 459–479, doi: 10.1016/S1367-9120(01)00039-6.

Catlos, E.J., Dubey, C.S., Harrison, T.M., and Edwards, M.A., 2004, Late Miocene movement within the Himalayan Main Central Thrust shear zone, Sikkim, northeast India: Journal of Metamorphic Geology, v. 22, p. 207–226, doi: 10.1111/j.1525-1314.2004.00509.x.

Cherniak, D.J., Watson, E.B., Grove, M., and Harrison, T.M., 2004, Pb diffusion in monazite: A combined RBS/SIMS study: Geochimica et Cosmochimica Acta, v. 68, p. 829–840, doi: 10.1016/j.gca.2003.07.012.

Cressey, G., Wall, F., and Cressey, B.A., 1999, Differential REE uptake by sector growth of monazite: Mineralogical Magazine, v. 63, p. 813–828, doi: 10.1180/002646199548952.

DeCelles, P.G., Gehrels, G.E., Quade, J., Ojha, T.P., Kapp, P.A., and Upreti, B.N., 1998, Neogene foreland basin deposits, erosional unroofing, and the kinematic history of Himalaya fold-thrust belt, western Nepal: Geological Society of America Bulletin, v. 110, p. 2–21, doi: 10.1130/0016-7606(1998)110<0002:NFBDEU>2.3.CO;2.

DeCelles, P.G., Robinson, D.M., Quade, J., Ojha, T.P., Garzione, C.N., Copeland, P., and Upreti, B.N., 2001, Stratigraphy, structure, and tectonic evolution of the Himalayan fold-thrust belt in western Nepal: Tectonics, v. 20, p. 487–509, doi: 10.1029/2000TC001226.

DeCelles, P.G., Robinson, D.M., and Zandt, G., 2002, Implications of shortening in the Himalayan fold-thrust belt for uplift of the Tibetan Plateau: Tectonics, v. 21, Art. No. 1062.

England, P.C., and Molnar, P., 1993, The interpretation of inverted metamorphic isograds using simple physical calculations: Tectonics, v. 12, p. 145–157.

England, P.C., Le Fort, P., Molnar, P., and Pêcher, A., 1992, Heat sources for Tertiary metamorphism and anatexis in the Annapurna-Manaslu region, central Nepal: Journal of Geophysical Research, v. 97, p. 2107–2128.

Evans, M.J., Derry, L.A., Anderson, S.P., and France-Lanord, C., 2001, Source of radiogenic Sr to Himalayan rivers: Geology, v. 29, p. 803–806, doi: 10.1130/0091-7613(2001)029<0803:HSORST>2.0.CO;2.

Ferry, J.M., 2000, Patterns of mineral occurrence in metamorphic rocks: American Mineralogist, v. 85, p. 1573–1588.

Ferry, J.M., and Spear, F.S., 1978, Experimental calibration of partitioning of Fe and Mg between biotite and garnet: Contributions to Mineralogy and Petrology, v. 66, p. 113–117, doi: 10.1007/BF00372150.

Fielding, E.J., 1996, Uplift and exhumation of metamorphic rocks: The Himalayan Tibet region: Tectonophysics, v. 260, p. 55–84, doi: 10.1016/0040-1951(96)00076-5.

Force, E.R., 1997, Geology and mineral resources of the Santa Catalina Mountains, southeastern Arizona: Tucson, Arizona, University of Arizona Press, p. 1–135.

Foster, G., Kinny, P., Vance, D., Prince, C., and Harris, N., 2000, The significance of monazite U-Th-Pb age data in metamorphic assemblages: A combined study of monazite and garnet chronometry: Earth and Planetary Science Letters, v. 181, p. 327–340, doi: 10.1016/S0012-821X(00)00212-0.

Franz, G., Andrehs, G., and Rhede, D., 1996, Crystal chemistry of monazite and xenotime from Saxothuringian-Moldanubian metapelites, NE Bavaria, Germany: European Journal of Mineralogy, v. 8, p. 1097–1118.

Ghosh, P., Padia, J.T., and Mohindra, R., 2004, Stable isotopic studies of palaeosol sediment from Upper Siwalik of Himachal Himalaya: Evidence for high monsoonal intensity during late Miocene?: Palaeogeography, Palaeoclimatology, Palaeoecology, v. 206, p. 103–114, doi: 10.1016/j.palaeo.2004.01.014.

Gilley, L.D., Harrison, T.M., Leloup, P.H., Ryerson, F.J., Lovera, O.M., and Wang, J.-H., 2003, Direct dating of left-lateral deformation along the Red River shear zone, China and Vietnam: Journal of Geophysical Research, v. 108, p. 2127–2148, doi: 10.1029/2001JB001726.

Guillot, S., Cosca, M., Allemand, P., and Le Fort, P., 1999, Contrasting metamorphic and geochronologic evolution along the Himalayan belt, *in* MacFarlane, A., et al., eds., Himalaya and Tibet: Mountain roots to mountain tops: Geological Society of America Special Paper 328, p. 117–128.

Harris, N.B.W., and Massey, J., 1994, Decompression and anatexis of Himalayan metapelites: Tectonics, v. 13, p. 1537–1546, doi: 10.1029/94TC01611.

Harris, N.B.W., Inger, S., and Massey, J., 1993, The role of fluids in the formation of High Himalayan leucogranites, *in* Trealor, P.J., and Searle, M.P., eds., Himalayan tectonics: Geological Society [London] Special Publication 74, p. 391–400.

Harris, N.B.W., Caddick, M., Kosler, J., Goswami, S., Vance, D., and Tindle, A.G., 2004, The pressure-temperature-time path of migmatites from the Sikkim Himalaya: Journal of Metamorphic Geology, v. 22, p. 249–264, doi: 10.1111/j.1525-1314.2004.00511.x.

Harrison, T.M., McKeegan, K.D., and Le Fort, P., 1995, Detection of inherited monazite in the Manaslu leucogranite by $^{208}Pb/^{232}Th$ ion microprobe dating: Crystallization age and tectonic implications: Earth and Planetary Science Letters, v. 133, p. 271–282, doi: 10.1016/0012-821X(95)00091-P.

Harrison, T.M., Grove, M., and Lovera, O.M., 1997, New insights into the origin of two contrasting Himalayan granite belts: Geology, v. 25, p. 899–902, doi: 10.1130/0091-7613(1997)025<0899:NIITOO>2.3.CO;2.

Harrison, T.M., Grove, M., Lovera, O.M., and Catlos, E.J., 1998, A model for the origin on Himalayan anatexis and inverted metamorphism: Journal of Geophysical Research, v. 103, p. 27,017–27,032, doi: 10.1029/98JB02468.

Harrison, T.M., Grove, M., Lovera, O.M., Catlos, E.J., and D'Andrea, J., 1999, The origin of Himalayan anatexis and inverted metamorphism: Models and constraints: Journal of Asian Earth Sciences, v. 17, p. 755–772, doi: 10.1016/S1367-9120(99)00018-8.

Harrison, T.M., Catlos, E.J., and Montel, J.-M., 2002, U-Th-Pb dating of phosphate minerals, *in* Hughes, J.M., et al., eds., Phosphates: Geochemical, geobiological and materials importance: Washington, D.C., Mineralogical Society of America Reviews in Mineralogy and Geochemistry, v. 48, p. 523–558.

Hodges, K.V., 2000, Tectonics of the Himalaya and southern Tibet from two perspectives: Geological Society of America Bulletin, v. 112, p. 324–350, doi: 10.1130/0016-7606(2000)112<0324:TOTHAS>2.3.CO;2.

Hodges, K.V., Parrish, R.R., and Searle, M.P., 1996, Tectonic evolution of the central Annapurna Range, Nepalese Himalayas: Tectonics, v. 15, p. 1264–1291, doi: 10.1029/96TC01791.

Hodges, K.V., Wobus, C., Ruhl, K., Schildgen, T., and Whipple, K., 2004, Quaternary deformation, river steepening, and heavy precipitation at the front of the Higher Himalayan ranges: Earth and Planetary Science Letters, v. 220, p. 379–389, doi: 10.1016/S0012-821X(04)00063-9.

Hoisch, T.D., 1990, Empirical calibration of six geobarometers for the mineral assemblage quartz + muscovite + biotite + plagioclase + garnet: Contributions to Mineralogy and Petrology, v. 104, p. 225–234, doi: 10.1007/BF00306445.

Hubbard, M.S., 1996, Ductile shear as a cause of inverted metamorphism: Example from the Nepal Himalaya: Journal of Geology, v. 104, p. 493–499.

Islam, R., Upadhyay, R., Ahmad, T., Thakur, V.C., and Sinha, A.K., 1999, Pan-African magmatism and sedimentation in the NW Himalayas: Gondwana Research, v. 2, p. 263–270, doi: 10.1016/S1342-937X(05)70150-7.

Jouanne, F., Mugnier, J.L., Gamond, J.F., Le Fort, P., Pandey, M.R., Bollinger, L., Flouzat, M., and Avouac, J.P., 2004, Current shortening across the Himalayas of Nepal: Geophysical Journal International, v. 157, p. 1–14, doi: 10.1111/j.1365-246X.2004.02180.x.

Kayal, J.R., 1996, Precursor Seismicity, foreshocks and aftershocks of the Uttarkashi earthquake of October 20, 1991 at Garhwal Himalaya: Tectonophysics, v. 263, p. 339–345.

Kingsbury, J.A., Miller, C.F., Wooden, J.L., and Harrison, T.M., 1993, Monazite paragenesis and U-Pb systematics in rocks of the eastern Mojave Desert, California, U.S.A.: Implications for thermochronometry: Chemical Geology, v. 110, p. 147–167, doi: 10.1016/0009-2541(93)90251-D.

Kohn, M.J., and Malloy, M.A., 2004, Formation of monazite via prograde metamorphic reactions among common silicates: Implications for age determinations: Geochimica et Cosmochimica Acta, v. 68, p. 101–113, doi: 10.1016/S0016-7037(03)00258-8.

Kohn, M.J., Wieland, M.S., Parkinson, C.D., and Upreti, B.N., 2004, Miocene faulting at plate tectonic velocity in the Himalaya of central Nepal: Earth and Planetary Science Letters, v. 228, p. 299–310, doi: 10.1016/j.epsl.2004.10.007.

Kohn, M.J., Wieland, M.S., Parkinson, C.D., and Upreti, B.N., 2005, Five generations of monazite in Langtang gneisses: Implications for chronology of the Himalayan metamorphic core: Journal of Metamorphic Geology, v. 23, p. 399–406, doi: 10.1111/j.1525-1314.2005.00584.x.

Lavé, J., and Avouac, J.P., 2000, Active folding of fluvial terraces across the Siwaliks Hills, Himalayas of central Nepal: Journal of Geophysical Research, v. 105, p. 5735–5770, doi: 10.1029/1999JB900292.

Le Fort, P., 1975, Himalaya, the collided range: Present knowledge of the continental arc: American Journal of Science, v. 275A, p. 1–44.

Le Fort, P., 1986, Metamorphism and magmatism during the Himalayan collision, *in* Coward, M.P., and Ries, A.C., eds., Collision tectonics: Geological Society [London] Special Publication 19, p. 159–172.

Le Fort, P., 1996, Evolution of the Himalaya, *in* Yin, A., and Harrison, T.M., eds., The tectonic evolution of Asia: Cambridge, UK, Cambridge University Press, p. 95–109.

Martin, A.J., DeCelles, P.G., Gehrels, G.E., Patchett, P.J., and Isachsen, C., 2005, Isotopic and structural constraints on the location of the Main Central Thrust in the Annapurna Range, central Nepal Himalaya: Geological Society of America Bulletin, v. 117, p. 926–944, doi: 10.1130/B25646.1.

Meigs, A.J., Burbank, D.W., and Beck, R.A., 1995, Middle-late Miocene (>10 Ma) formation of the Main Boundary Thrust in the western Himalaya: Geology, v. 23, p. 423–426, doi: 10.1130/0091-7613(1995)023<0423:MLMMFO>2.3.CO;2.

Meldrum, A., Boatner, L.A., Weber, W.J., and Ewing, R.C., 1998, Radiation damage in zircon and monazite: Geochimica et Cosmochimica Acta, v. 62, p. 2509–2520, doi: 10.1016/S0016-7037(98)00174-4.

Metcalfe, R.P., 1993, Pressure, temperature and time constraints on metamorphism across the Main Central Thrust zone and High Himalaya slab in the Garhwal Himalaya, *in* Trealor, P.J., and Searle, M.P., eds., Himalayan tectonics: Geological Society [London] Special Publication 74, p. 485–509.

Miller, C., Klotzli, U., Thoni, F.W., and Grasemann, B., 2000, Proterozoic crustal evolution in the NW Himalaya (India) as recorded by circa 1.80 Ga mafic and 1.84 Ga granitic magmatism: Precambrian Research, v. 103, p. 191–206, doi: 10.1016/S0301-9268(00)00091-7.

Montel, J., Kornprobst, J., and Vielzeuf, D., 2000, Preservation of old U-Th-Pb ages in shielded monazite: Example from Beni Bousera Hercynian kinzigites (Morocco): Journal of Metamorphic Geology, v. 18, p. 335–342, doi: 10.1046/j.1525-1314.2000.00261.x.

Nelson, K.D., Zhao, W., Brown, L.D., Kuo, J., Che, J., Liu, X., Klemperer, S.L., Makovsky, Y., Meissner, R., Mechie, J., Kind, R., Wenzel, F., Ni, J., Nabelek, J., Chen, L., Tan, H., Wei, W., Jones, A.G., Booker, J., Unsworth, M., Kidd, W.S.F., Hauck, M., Alsdorf, D., Ross, A., Cogan, M., Wu, C., Sandvol, E.A., and Edwards, M., 1996, Partially molten crust beneath southern Tibet: Synthesis of project INDEPTH results: Science, v. 274, p. 1684–1688, doi: 10.1126/science.274.5293.1684.

Ni, J., and Barazangi, 1984, Seismotectonics and the Himalayan Collision Zone: Geometry of the underthrusting Indian plate beneath the Himalaya: Journal of Geophysical Research, v. 89, p. 1147–1163.

Noble, S.R., and Searle, M.P., 1995, Age of crustal melting and leucogranite formation from U-Pb zircon and monazite dating in the western Himalaya, Zanskar, India: Geology, v. 23, p. 1135–1138, doi: 10.1130/0091-7613(1995)023<1135:AOCMAL>2.3.CO;2.

Oldham, R.D., 1883, Note on the geology of Jaunsar and the lower Himalayas: Memoirs of the Geological Survey of India, v. 3, p. 193–198.

Overstreet, W.C., 1967, The geologic occurrence of monazite: U.S. Geological Survey Professional Paper 530, p. 1–327.

Parrish, R.R., 1990, U-Pb dating of monazite and its application to geological problems: Canadian Journal of Earth Sciences, v. 27, p. 1431–1450.

Pêcher, A., 1989, The metamorphism in the central Himalaya: Journal of Metamorphic Geology, v. 7, p. 31–41.

Pêcher, A., and Scaillet, B., 1989, La structure du Haut-Himalaya au Garhwal (Indes): Eclogae Geologicae Helvetiae, v. 82, p. 655–668.

Powers, P.M., Lillie, R.J., and Yeats, R.S., 1998, Structure and shortening of the Kangra and Dehra Dun reentrants, sub-Himalaya, India: Geological Society of America Bulletin, v. 110, p. 1010–1027, doi: 10.1130/0016-7606(1998)110<1010:SASOTK>2.3.CO;2.

Pyle, J.M., and Spear, F.S., 1999, Yttrium zoning in garnet: Coupling of major and accessory phases during metamorphic reactions: Geological Materials Research, v. 1, p. 1–36.

Pyle, J.M., and Spear, F.S., 2003, Four generations of accessory-phase growth in low-pressure migmatites from SW New Hampshire: American Mineralogist, v. 88, p. 338–351.

Pyle, J.M., Spear, F.S., Rudnick, R.L., and McDonough, W.F., 2001, Monazite-xenotime-garnet equilibrium in metapelites and a new monazite-garnet thermometer: Journal of Petrology, v. 42, p. 2083–2107, doi: 10.1093/petrology/42.11.2083.

Pyle, J.M., Spear, F.S., Cheney, J.T., and Layne, G., 2005, Monazite ages in the Chesham Pond Nappe, SW New Hampshire, U.S.A.: Implications for assembly of central New England thrust sheets: American Mineralogist, v. 90, p. 592–606, doi: 10.2138/am.2005.1341.

Robinson, D.M., DeCelles, P.G., Garizone, C.N., Pearson, O.N., Harrison, T.M., and Catlos, E.J., 2003, Kinematic model for the Main Central Thrust in Nepal: Geology, v. 31, p. 359–362, doi: 10.1130/0091-7613(2003)031<0359:KMFTMC>2.0.CO;2.

Royden, L.H., 1993, The steady-state thermal structure of eroding orogenic belts and accretionary prisms: Journal of Geophysical Research, v. 98, p. 4487–4507.

Sarkar, I., Pachauri, A.K., and Israil, M., 2001, On the damage caused by the Chamoli earthquake of 29 March, 1999: Journal of Asian Earth Sciences, v. 19, p. 129–134, doi: 10.1016/S1367-9120(00)00021-3.

Sarkar, S.C., Chernyshev, I.V., and Banerjee, H., 2000, Mid-Proterozoic Pb-Pb ages for some Himalayan base-metal deposits and comparison to deposits in Rajasthan, NW India: Precambrian Research, v. 99, p. 171–178, doi: 10.1016/S0301-9268(99)00057-1.

Schelling, D., and Arita, K., 1991, Thrust tectonics, crustal shortening, and the structure of the far-eastern Nepal Himalayas: Tectonics, v. 10, p. 851–862.

Searle, M.P., and Godin, L., 2003, The South Tibetan Detachment and the Manaslu leucogranite: A structural reinterpretation and restoration of the Annapurna-Manaslu Himalaya, Nepal: Journal of Geology, v. 111, p. 505–535, doi: 10.1086/376763.

Searle, M.P., and Rex, A.J., 1989, Thermal model for the Zanskar Himalaya: Journal of Metamorphic Geology, v. 7, p. 127–134.

Searle, M.P., Parrish, R.R., Hodges, K.V., Hurford, A.J., Ayres, M.W., and Whitehouse, M.J., 1997, Shisha-Pangma leucogranite, South Tibetan Himalaya: Field relations, geochemistry, age, origin, and emplacement: Journal of Geology, v. 105, p. 295–317.

Searle, M.P., Noble, S.R., Hurford, A.J., and Rex, D.C., 1999, Age of crustal melting, emplacement and exhumation history of the Shivling leucogranite, Garhwal Himalaya: Geological Magazine, v. 136, p. 513–525, doi: 10.1017/S0016756899002885.

Seeber, L., and Gornitz, V., 1983, River profiles along the Himalayan arc as indicators of active tectonics: Tectonophysics, v. 92, p. 335–367, doi: 10.1016/0040-1951(83)90201-9.

Seeber, L., Armbruster, J.G., and Quittmeyer, R., 1981, Seismicity and continental subduction in the Himalayan arc, *in* Gupta, H.K., and Delany, F.M., eds., Zagros, Hindu Kush, Himalayan Geodynamic Evolution: Washington, D.C., American Geophysical Union Geodymanics Series, v. 3, p. 215–242.

Smith, H.A., and Barreiro, B., 1990, Monazite U-Pb dating of staurolite-grade metamorphism in pelitic schists: Contributions to Mineralogy and Petrology, v. 105, p. 602–615, doi: 10.1007/BF00302498.

Spear, F.S., and Kohn, M.J., 2001, Program GTB: GeoThermoBarometry: Rensselaer Polytechnic Institute, http://ees2.geo.rpi.edu/MetaPetaRen/GTB_Prog/GTB.htmll, last accessed 11 December 2006.

Spear, F.S., and Pyle, J.M., 2002, Apatite, monazite, and xenotime in metamorphic rocks, *in* Hughes, J.M., et al., eds., Phosphates: Geochemical, geobiological and materials importance: Washington, D.C., Mineralogical Society of America Reviews in Mineralogy and Geochemistry, v. 48, p. 293–335.

Srivastava, P., and Mitra, G., 1994, Thrust geometries and deep structure of the outer and Lesser Himalaya Kumaon and Garhwal (India): Implications for evolution of the Himalayan fold-and-thrust belt: Tectonics, v. 13, p. 89–109, doi: 10.1029/93TC01130.

Stacey, J.S., and Kramers, J.D., 1975, Approximate of terrestrial lead isotope evolution by a two-stage model: Earth and Planetary Science Letters, v. 26, p. 207–221, doi: 10.1016/0012-821X(75)90088-6.

Stephenson, B.J., Searle, M.P., Waters, D.J., and Rex, D.C., 2001, Structure of the Main Central Thrust zone and extrusion of the High Himalayan deep crustal wedge, Kishtwar-Zanskar Himalaya: Geological Society [London] Journal, v. 158, p. 637–652.

Tapponnier, P., Peltzer, G., LeDain, A.Y., Armijo, R., and Cobbold, P., 1982, Propagating extrusion tectonics in Asia: New insights from simple experiments with plasticine: Geology, v. 10, p. 611–616, doi: 10.1130/0091-7613(1982)10<611:PETIAN>2.0.CO;2.

Tapponnier, P., Zhiqin, X., Roger, F., Meyer, B., Arnaud, N., Wittlinger, G., and Jingsui, Y., 2001, Oblique stepwise rise and growth of the Tibet Plateau: Science, v. 294, p. 1671–1677, doi: 10.1126/science.105978.

Townsend, K.J., Miller, C.F., D'Andrea, J.L., Ayers, J.C., Harrison, T.M., and Coath, C.D., 2001, Low-temperature replacement of monazite in the Ireteba granite, southern Nevada: Geochronological implications: Chemical Geology, v. 172, p. 95–112, doi: 10.1016/S0009-2541(00)00238-2.

Upreti, B.N., 1999, An overview of the stratigraphy and tectonics of the Nepal Himalaya: Journal of Asian Earth Sciences, v. 17, p. 577–606, doi: 10.1016/S1367-9120(99)00047-4.

Valdiya, K.S., 1992, The Main Boundary Thrust zone of the Himalaya, India: Annales Tectonicae, v. 6, supplement, p. 54–84.

Valdiya, K.S., 1995, Proterozoic sedimentation and Pan-African geodynamic development in the Himalaya: Precambrian Research, v. 74, p. 35–55, doi: 10.1016/0301-9268(95)00004-O.

Vannay, J.C., and Steck, A., 1995, Tectonic evolution of the High Himalaya in Upper Lahul (NW Himalaya, India): Tectonics, v. 14, p. 253–263, doi: 10.1029/94TC02455.

Virk, H.S., and Walia, V., 2001, Helium/radon precursory signals of Chamoli earthquake, India: Radiation Measurements, v. 34, p. 379–384, doi: 10.1016/S1350-4487(01)00190-1.

Wiesmayr, G., and Grasemann, B., 2002, Eohimalayan fold-and-thrust belt: Implications for the geodynamic evolution of the NW Himalaya (India): Tectonics, v. 21, 8 p.

Wing, B.A., Ferry, J.M., and Harrison, T.M., 2003, Prograde destruction and formation of monazite and allanite during contact and regional metamorphism of pelites; petrology and geochronology: Contributions to Mineralogy and Petrology, v. 145, p. 228–250.

Yeats, R.S., Nakata, T., Farah, A., Fort, M., Mirza, M.A., Pandey, M.R., and Stein, R.S., 1992, The Himalayan frontal fault system: Annales Tectonicae, v. 6, supplement, p. 85–98.

Yin, A., and Harrison, T.M., 2000, Geologic evolution of the Himalayan-Tibetan orogen: Annual Review of Earth and Planetary Sciences, v. 28, p. 211–280, doi: 10.1146/annurev.earth.28.1.211.

Yin, A., Harrison, T.M., Murphy, M.A., Grove, M., Nie, S., Ryerson, F.J., Feng, W.X., and Le, C.Z., 1999, Tertiary deformation history of southeastern and southwestern Tibet during the Indo-Asian collision: Geological Society of America Bulletin, v. 111, p. 1644–1664, doi: 10.1130/0016-7606(1999)111<1644:TDHOSA>2.3.CO;2.

Zhu, X.K., and O'Nions, R.K., 1999, Monazite chemical composition: Some implications for monazite geochronology: Contributions to Mineralogy and Petrology, v. 137, p. 351–363, doi: 10.1007/s004100050555.

Manuscript Accepted by the Society 13 July 2006